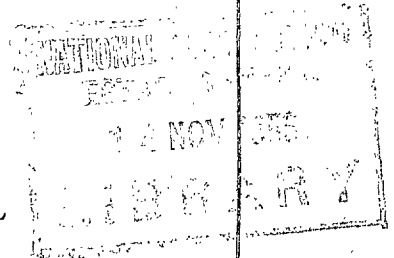




MINISTRY OF SUPPLY

AERONAUTICAL RESEARCH COUNCIL
REPORTS AND MEMORANDA



The Manoeuvrability of Aircraft in Circling Flight

By

H. L. PRICE, Ph.D.

of the University of Leeds
formerly with Messrs. Blackburn Aircraft, Ltd.

Crown Copyright Reserved

LONDON : HER MAJESTY'S STATIONERY OFFICE

1955

PRICE 8s 6d NET

The Manoeuvrability of Aircraft in Circling Flight

By

H. L. PRICE, Ph.D.

of the University of Leeds
formerly with Messrs. Blackburn Aircraft, Ltd.

*Reports and Memoranda No. 2838**

May, 1952

Summary.—An investigation is made into the manoeuvre of an aeroplane in the entry into and recovery from a true banked horizontal turn executed without sideslip or loss of height, and the proper continuous co-ordination of aileron, elevator and rudder is deduced for all stages of the manoeuvre. It is shown that the rolling motion is practically unaffected by the other modes of motion, enabling the kinematics of the rolling mode to be solved in terms solely of the applied aileron movement or stick force. The aileron is regarded as the prime initiator of the turn, operated in some pre-chosen manner, and the elevator and rudder loads are expressed as functions of the determinable rolling velocity and acceleration. The loads to trim in the final steady turn are found as a particular case.

Several different forms of aileron operation are examined, including a family in which the maximum value of the rolling velocity (or helix-angle in roll) is stipulated beforehand. The co-ordinating elevator load may, in adverse cases, attain peak values considerably in excess of the final load to trim, and the dependence of such peaks on the manner of aileron control operation is examined. It is shown that rapid entries into a turn demanding large rolling velocities at high altitudes are likely to require a large pull back of the stick, followed by a hasty push forward. In order to ensure that the elevator co-ordination should consist of a steady one-way movement of the stick, it is necessary that the aileron be applied in such a way that maximum rolling velocity be obtained when the angle of bank is small.

Two manoeuvrability criteria are suggested for the entry into the turn, the first relating the final elevator load to the amount of g generated, and the second relating maximum aileron load to the maximum required rolling velocity and final angle of bank. Extensive information regarding this rolling aspect of the manoeuvre is presented in a set of charts using non-dimensional parameters.

The mathematical analysis is contained in appendices.

1. *The Nature of the Manoeuvre and the Basic Physical Assumptions.*—The problem investigated in this report is the three-dimensional manoeuvre of an aeroplane in the transition from steady horizontal symmetric flight into a steady horizontal turn at an assigned angle of bank. The manoeuvre may be as violent as the controls will allow, and particular attention is paid to the manner in which the several controls must be kept in step. The term 'co-ordination' is normally used in some loose way to describe such a process, but a precise definition of co-ordination will later be given in order to eliminate any ambiguity.

The kinematics of the manoeuvre describing the velocities and angular velocities of the aeroplane, fall into three distinct phases. The first and third are the initial and final steady stages, which reasonably may be supposed to be without sideslip, while the intermediate phase consists of the unsteady transitional motion comprising the manoeuvre proper. As distinct from longitudinal manoeuvrability theory, due attention is paid here to the precise manner in which the final steady stage is reached, so that while the final loads to trim are fixed quantities

* Revised version of original report dated January, 1945.

depending on the final angle of bank, the actual rolling transition may be performed as slowly or as quickly as desired. The differences in the kinematics are reflected in the totally different kinds of intermediate control loads which are correspondingly required.

Each co-ordinated manoeuvre represents a particular way of executing the required turn, but the act of co-ordination may be more difficult to perform in some cases than in others. Failure to co-ordinate the controls may result in an undue amount of sideslip or loss of height, and the mere movement of the controls straight to their final trim values (generally demanding quite small deflections), will not in itself guarantee that the aircraft will take up the appropriate steady turning motion, particularly if the angle of bank is large. If the manoeuvre is to be achieved with any rapidity at all, substantial rolling velocities will be demanded, which in turn entails large aileron angles for some period during the transition—large, that is, compared with the final steady value. The ailerons at least, then, will perform some large excursion, and consequently may be looked upon as the dominant control. ‘Co-ordination’ may then be interpreted as the keeping in step of the elevator and rudder with whatever motion is dictated by the ailerons, and will take a variety of forms depending upon how much sideslip or change in height is desired. A *unique* co-ordination is defined if it is stipulated that there should be no sideslip or loss of height throughout the transition, whatever aileron operation be adopted. This will be a basic assumption of the present work.

One additional assumption may be made that there is no loss of speed during the manoeuvre. This cannot strictly be justified because in the final steady state the aircraft incidence will have been increased, and the speed will have dropped in the absence of a compensating increase in thrust. Typical rolling transitions will be virtually completed, however, in a matter of a second or two, and as the only retarding force is the increased drag, negligible speed losses will ensue. Alternatively, constancy of speed may be postulated exactly, and the necessary thrust changes deduced as a further control co-ordination.

2. *Outline of the Method, and the Basic Analytical Assumptions.*—The essence of the analytical method of solving the problem is to leave the angle of bank ϕ as some unspecified function of time and only in the final stage to assign to it a time variation appropriate to the particular aileron operating technique. The remaining kinematic variables are then solved as functions of ϕ and its rate of change, following which the control loads may be expressed in terms of ϕ and the stability derivatives.

In order to examine the feasibility of the method and to understand the assumptions involved, consider the form of the general equations of motion. Using the standard system of moving axes there are four basic types of equations, namely

(a) the three equations of resolution along the axes, involving $u, w; p, q, r; \theta, \phi, \psi$ and the control displacement terms $y_{\xi}\zeta$ and $z_{\eta}\eta$

(Note: v is absent on the assumption that sideslip is maintained identically zero)

(b) the three equations of moments, involving $u, w; p, q, r;$ and the control moments $l_{\xi}\xi, m_{\eta}\eta,$ etc.

(c) the three geometrical relationships between p, q, r and θ, ϕ, ψ

(d) the single geometrical equation between w, θ and ϕ expressing constancy of height.

Now ideally the function of a control surface is to produce a moment about the centre of gravity, and the fact that in the case of the elevator and rudder there is also an unbalanced normal force may merely be regarded as accidental*. At any rate the terms $y_{\xi}\zeta$ and $z_{\eta}\eta$ are generally omitted outright from ordinary stick-free stability calculations, and a similar omission will be made here, though only after an examination of the error involved. Groups (a), (c) and (d) will then

* The rudder, however, may be required to generate sideslip deliberately, and does so by means of the side force.

consist of seven equations in eight variables alone, *viz.*, $u, w; \theta, \phi, \psi; \dot{p}, q, r$, and therefore each of the seven variables $u, w; \theta, \psi; \dot{p}, q, r$ can be expressed in terms of ϕ . Their values can then be substituted in the elevator and rudder moment equations (group (b)) and the co-ordinating control angles deduced as functions of ϕ .

For a given aileron operation the determination of ϕ as a function of time at first sight seems rather involved. The appropriate moment equation, sideslip being zero, is, in non-dimensional form

$$i_A \dot{\bar{p}} - (i_B - i_C) \bar{q} \bar{r} - l_p \bar{p} - l_r \bar{r} = \mu l_\xi \xi(t) \quad \dots \quad \dots \quad \dots \quad \dots \quad (1)$$

where t also is measured in non-dimensional units.

Now in this it can be shown *a posteriori* that even for the largest variations in ϕ , the influence of the \bar{q} and \bar{r} terms is negligible. It can further be shown that in this equation \bar{p} can be replaced by $\dot{\bar{p}}$. The reduced equation accordingly involves only ϕ , its derivatives and the known time function $\xi(t)$, and so can readily be solved.

It must be stressed that the manoeuvre is not regarded here as an extended case of a 'stability' type disturbance, the theory of which is based on the notion of *infinitesimal* displacements. Ordinarily the stability approach to manoeuvrability problems does give approximately correct results even for moderately large excursions in the variables. It suffers, however, from the defect that product terms, for example, are always rejected outright. Now the unapproximated equations of motion, such as the one given above, do contain product terms in the variables arising from two sources. Firstly there are the kinematic products such as $\bar{w} \bar{p}, \bar{q} \bar{r}$, which enter on account of the rotation of the axes, and secondly there are terms involving stability derivatives. These consist of the explicit first order quantities like $l_r \bar{r}$ and the implicit higher order terms like $l_p \bar{p} \dot{\bar{p}}$. The latter are invariably neglected, and there is reason to believe they are unimportant here. A term like $l_r \bar{r}$, however, normally regarded as first order, has an additional contribution due to the fact that l_r is proportional to incidence, which in the present manoeuvre generally undergoes a substantial increase. This variation is here taken into account, and to do so the further assumption is made that there is no time lag between an increase in angle of incidence and the corresponding lift increment on the wing section.

3. *Formulae for the Control Co-ordination: Dynamic and Static Values.*—The analytical expressions for the control displacements involve certain simple trigonometrical functions of ϕ , which, in practice, may be tabulated once and for all. They are

$$\begin{aligned} q_1 &\equiv (\sec \phi - \cos \phi), & q_2 &\equiv \sec \phi \tan \phi, \\ r_1 &\equiv \sin \phi, & r_2 &\equiv \sec \phi - 1. \end{aligned}$$

The control angles are then given by

$$\frac{\mu l_\xi}{i_A} \xi(t) = \dot{\bar{p}} - \frac{l_p}{i_A} \bar{p} - \frac{C_L l_r}{2 i_A} \sec \phi \left(r_1 + r_2 \frac{2 \bar{p}}{a} \right) \quad \dots \quad \dots \quad \dots \quad \dots \quad \dots \quad (2)$$

$$\frac{\mu m_\eta}{i_B} \eta(t) = \frac{C_L}{2} \left\{ \frac{2 q_2}{a} \dot{\bar{p}} + \bar{p} \left[\frac{d q_1}{d \phi} + \frac{2 \bar{p}}{a} \frac{d q_2}{d \phi} - \frac{2 q_2}{a} \left(\frac{\mu m_w}{i_B} + m_q \right) \right] - \left(\frac{\mu m_w}{i_B} \frac{2 r_2}{a} + \frac{m_q}{i_B} q_1 \right) \right\} \dots \quad (3)$$

$$\frac{\mu n_\zeta}{i_C} \zeta(t) = \frac{C_L}{2} \left\{ \frac{2 r_2}{a} \dot{\bar{p}} + \bar{p} \left[\frac{d r_1}{d \phi} + \frac{2 \bar{p}}{a} \frac{d r_2}{d \phi} - \frac{2}{i_C} \left(\frac{n_p \sec \phi}{C_L} + \frac{n_r r_2}{a} \right) \right] - \left(\frac{n_r}{i_C} r_1 + \frac{\mu n_\xi}{i_C} \xi \frac{2}{C_L} \right) \right\} \quad (4)$$

where $a \equiv dC_L/d\alpha$ and C_L, l_r, n_p are calculated at the original incidence.

The expressions on the right-hand sides of these equations fall naturally into two parts, those dependent and those independent of \bar{p} , the rolling velocity. The contributions to the control angles made by the \bar{p} terms may aptly be called the 'dynamic' control displacements since they

5. *Methods for Obtaining ϕ Variations.*—There are two processes by which suitable expressions may be obtained for \bar{p} and ϕ in terms of the independent time variable. The first process consists simply of prescribing a likely form of $\phi - t$ variation, based possibly on flight test results, and the second process consists of those methods wherein either the aileron angle or aileron load variation is prescribed and the \bar{p} and ϕ variation deduced.

In the first class the boundary conditions are that ϕ , \bar{p} ($= d\phi/dt$) and $\dot{\bar{p}}$ should vanish initially, and that \bar{p} and $\dot{\bar{p}}$ should be zero at the final angle of bank. Also, if the final angle of bank is obtained without an overshoot, \bar{p} will always be of the same sign. The shape of the \bar{p} vs. t curve, then, is such that, starting initially tangential to the t -axis, it attains some peak value \bar{p}_{\max} at some intermediate point of the manoeuvre before returning to the t -axis, either asymptotically, or else tangentially at a finite point. The asymptotic case arises when exponential expressions are used to describe ϕ , and also when the simplified rolling equation

$$\dot{\bar{p}} - \frac{l_p}{i_A} \bar{p} = \frac{\mu l_\xi}{i_A} \xi(t) \quad \dots \quad \dots \quad \dots \quad \dots \quad \dots \quad \dots \quad \dots \quad (7)$$

is used with chosen expressions for $\xi(t)$. The final angle of bank is then strictly obtained only after an infinite length of time, and on this account will be denoted by ϕ_∞ . The same symbol, however, will also be used even when, in other cases, it may be reached in a finite period of time.

The basic geometric feature of the \bar{p} vs. t curve is that the area between it and the t -axis is proportional to ϕ_∞ . It follows, therefore, that overshooting ϕ_∞ in general leads to a slower overall time for the manoeuvre because of the negative values of \bar{p} required to bring the aircraft back. This is in direct contrast to the case of the pull out from a dive at a given normal acceleration, for which the *non*-overshoot case represents the slowest manoeuvre.

Equation (7) shows that effectively the rolling equation is no different from the rolling equation as used in discussing simple rolling performance. Here, however, the actual rolling manoeuvre is different, demanding the ability not only to generate a large value of $\bar{p}b/2U_0$ (the helix angle in roll) but also of checking it within the compass of a given final angle of bank. The manoeuvre may in fact be specified 'geometrically' *via* the \bar{p} vs. t curve in terms of ϕ_∞ , the maximum required value of $\bar{p}b/2U_0$, and also the instant during the manoeuvre at which this peak rolling velocity is to be attained. This leads to the following two types of ϕ or \bar{p} analysis:

(A.1) An exploratory 'Synthetic' method in which the $\phi - t$ variation, based on actual flight results, is taken as

$$\phi = \phi_\infty(1 - e^{-x^n})$$

where $x = ht$ and n and h are parameters.

(A.2.) The 'Rolling Velocity' method in which the \bar{p} vs. t curve is regarded as being built up of four successive generalised parabolic-arcs enabling the magnitude and instant of the peak rolling velocity to be assigned.

The second class of solution is based on prescribing the form of the aileron operation, and is itself divisible into two classes as follows:

(B.1.) The 'Aileron-Angle' method, in which the ξ vs. t curve is built up of successive linear sections. (Alternatively the aileron load could be specified.)

(B.2.) The 'Aileron-Helix-Angle' method, in which ϕ_∞ and \bar{p}_{\max} are specified and also, the *shape* (but not size) of the aileron load versus time curve.

6. *Elevator Co-ordination for the 'Synthetic' Method.*—The initial numerical work of the theory was carried out by assigning a suitable value to the parameter n in the formula

$$\phi = \phi_\infty(1 - e^{-x^n}).$$

The value 2.1 was chosen so as to give very close agreement with a rolling-velocity curve obtained

in flight tests of a *Spitfire* in a 3g turn ($\phi = 70.53$ deg) at an altitude of 6000 ft at 250 m.p.h. A.S.I. (Fig. 1). The theoretical peak rolling velocity was arranged to be equal to the actual measured value, given by

$$\left(\frac{pb}{2U_0}\right)_{\max} = 0.0449.$$

The theoretical co-ordinating elevator load is shown in curve (a) of Fig. 2, and it is seen that it increases monotonically to its final steady value. (Note: Discrepancy with the measured value in Fig. 1 may be attributed in part at least to some uncertainty in the values of b_1 and b_2 for the elevator.)

Curve (b) shows the effect of mass-balancing the elevator to the extent of arranging for its centre of gravity to lie on the hinge-line, the result being a general reduction, but also overshoot and reversal, in load.

Curve (c) shows the effect of doubling the peak rolling velocity. This demands a very large increase in the 'dynamic' elevator load, and as a consequence introduces a well-defined peak in the co-ordinating elevator load.

Curve (d) shows the same load peaking phenomenon, but in a much aggravated form, resulting from a simultaneous increase in the maximum rolling velocity and altitude.

The disturbing feature of these curves is the enormous increase in the 'dynamic' elevator load due to increasing either the peak rolling velocity or the altitude. Reversal co-ordinations of this type are obviously very difficult to perform accurately, and it is therefore important to discover whether suitable aileron operations can be found which will yield simple elevator co-ordinations. For this purpose it will only be necessary to make brief reference to method (B.1), but method (B.2) will be dealt with in some detail. This will indicate the steps necessary to ensure simplified co-ordination, after which a return will be made to method (A.2) to confirm in a general way the findings of method (B.2).

7. *The 'Aileron-Angle' Method.*—The chief use to which the 'aileron-angle' method has been put has been to examine the validity of neglecting the yawing term $l_r\bar{r}$ in the rolling equation (1). Fig. 3 shows the calculated aileron angles required to produce a 3g turn, the shape of the ξ vs. t curve being based on an actual *Spitfire* manoeuvre. In the curve $OA_1A_2A_3A_4$, yawing is neglected altogether, while in curve $OA_1'A_2'A_3'A_4'$ a correction is made to ξ by inserting the term $l_r\bar{r}$. Here the value of \bar{r} has been calculated to a first approximation from equation (38) of Appendix I, *viz.*,

$$\bar{r} = \frac{1}{2} C_L(\alpha_0) \left[\sin \phi + (\sec \phi - 1) \frac{2}{a} \bar{p} \right]$$

using the values of ϕ and \bar{p} previously obtained from the simplified rolling equation. It is immediately obvious from the figure that the yawing effect is quite negligible except in the ultimate stages of the manoeuvre, where the final steady aileron rolling moment is in any case required to nullify the wing rolling moment $l_r\bar{r}$ due to steady yawing.

8. *The 'Aileron-Helix-Angle' Method.*—8.1. *The Rolling Aspect.*—In the 'aileron-helix-angle' method a choice of three shapes is assigned to the curves of aileron stick load against time, namely:

- (a) An isosceles triangle with base on the horizontal t -axis (triangular loading), the aileron being applied for, say, time $2t_1$.
- (b) A trapezium with base on the t -axis, having equal period of increasing, constant, and decreasing stick load (trapezoidal loading), the aileron being applied for, say, time $3t_1$.
- (c) A parabola with axis perpendicular to the t -axis (parabolic loading), the aileron being applied for, say, time t_1 .

In addition to the shape of the curve, the values of ϕ_∞ and of the maximum required helix angle in roll, $(pb/2U_0)_{\max}$ are specified beforehand.

A most valuable feature of the method is that the magnitude and duration of the aileron load required for the manoeuvre may be read off directly from completely generalised charts. The values of \bar{p} and ϕ are also readily obtainable for substitution in the expression for the co-ordinating elevator load. The method may in fact be regarded as providing, incidentally, a rolling performance criterion of an extended kind. Thus whereas one conventional rolling performance criterion is concerned merely with the ability of an aeroplane to generate an assigned peak rolling velocity without regard to the time taken for it to be achieved, the manoeuvres described above do take into account both rolling accelerations and retardations, and to that extent are more realistic.

8.2. *The Analytical Results.*—The solutions to the rolling motion in the cases (a), (b) and (c) above are based on the simplified rolling equation

$$\ddot{\bar{p}} + h'\dot{\bar{p}} = \frac{\mu l_{\xi}}{i_A} \cdot \frac{C_H}{2b_2} \quad \left(\bar{p} = \mu \frac{\dot{\phi} b}{2U_0} \right)$$

where

$$h' = -\frac{l_p}{i_A} \left(1 + \frac{l_{\xi} b_1}{l_p b_2} \right).$$

At the instant when the prescribed maximum rolling velocity is attained, $\dot{\bar{p}}$ is zero, and denoting the aileron load at that instant by \bar{P} , its value is given directly by

$$\bar{P} = mb_2 h' i_A \left(\frac{\dot{\phi} b}{2U_0} \right)_{\max} \rho S_{\xi} c_{\xi} U_0^2 / l_{\xi}$$

where m is the gearing factor converting hinge moment to stick force. This value of the stick load *has* to be obtained whatever the piloting technique, and is the minimum aileron load capable of satisfying the kinematics of the manoeuvre. Now because the shapes of the load-time curves are prescribed, it is only necessary for their complete determination to find the maximum value P_{\max} of the aileron load, and the duration $2t_1$, $3t_1$ or t_1 of the load in the individual cases (a), (b), (c). The solutions of the problem are displayed in Charts (I), (II), (III) which show the value of P_{\max}/\bar{P} plotted against a parameter A defined by the relation

$$A \equiv \frac{\mu}{h' \phi_{\infty}} \left(\frac{\dot{\phi} b}{2U_0} \right)_{\max} \text{ i.e., } \left(\frac{\dot{\bar{p}}_{\max}}{h' \phi_{\infty}} \right).$$

In addition the duration of the load is obtained in terms of a parameter X defined by $X \equiv h't_1$. The analytical formulae from which the charts are derived are as given below, while the actual solution for case (a) is derived in Appendix II.

Case (a)

$$\frac{P_{\max}}{\bar{P}} = \frac{1}{AX} \text{ where } A = \frac{1}{X} - \frac{1}{X^2} \log_e (2 - e^{-X})$$

Case (b)

$$\frac{P_{\max}}{\bar{P}} = \frac{1}{2AX} \text{ where } A = \frac{1}{2X} - \frac{1}{2X^2} \log_e (1 + e^{-X} - e^{-2X})$$

Case (c)

$$\frac{P_{\max}}{\bar{P}} = \frac{3}{2AX} \text{ where } X \text{ is given by the elimination of the parameter } k \text{ from the}$$

two equations

$$A = \frac{6k(1-k)}{X}, \quad X = \frac{2kX}{(1 - e^{-kX})} - 2.$$

In a practical case the value of A is determined from the known boundary conditions, and the corresponding values of X and P_{\max}/\bar{P} are read off from the appropriate chart.

It is possible to determine the relative merits of the aileron techniques (a), (b), (c) by finding which technique demands the smallest value of P_{\max} for a given value of A . The result is shown in Fig. 4, whence it is seen that the order of preference is trapezium, then parabolic, then triangular aileron loading.

8.3. *Elevator Co-ordination.*—For the purpose of comparison with the ‘synthetic’ method the co-ordinating elevator load is worked out for the same boundary conditions, namely a 3g turn at 250 m.p.h. A.S.I. at 27,000 ft, achieving a peak value 0.08984 for the helix-angle in roll. Two cases are considered, corresponding to triangular and parabolic aileron loading, and the co-ordinating elevator loads are shown in Figs. 5 and 6. It is at once apparent that the elevator peaks have disappeared. This gratifying feature indicates that a smooth control co-ordination is possible even for the more adverse kinematical conditions, and one deduces that the phenomenon of peaking co-ordination is not one ‘built-in’ to the aeroplane, but is a consequence of the particular aileron operating technique adopted. It is not in fact difficult to give a physical explanation of the phenomenon.

9. *The Origin of the Peak Loads.*—Consider Fig. 7, showing the growth of rolling velocity and angle of bank plotted against time for two aileron techniques corresponding to the triangular loading case (a), and the ‘synthetic’ method case with $n = 2.9$. The chief point of difference is that in the first case the large rolling velocities occur for an angle of bank of about 20 deg, and in the second case for an angle of 40 deg. Now in order that the aircraft should maintain height during the manoeuvre, the vertical component of the lift force, $L \cos \phi \cos \theta$, must remain substantially unaltered. In order to ensure this at a given rolling velocity, the rate of growth of the total lift vector—and therefore also of incidence—will have to be greater, the greater the angle of bank. Consequently, quicker and also larger changes in elevator load are required if the largest rolling velocities occur when the angle of bank is already large. The increase in incidence, however, can only be imparted by a correspondingly rapid angular acceleration of the aeroplane, followed by an angular retardation. This in turn demands substantial elevator movement to overcome the damping and inertia in pitch. But irrespective of the intermediate control loads, the final value to trim is limited, being dictated solely by the steady conditions in the turn. Hence a peak is induced in the elevator load on account of the large rolling velocities occurring only late in the manoeuvre.

It is also easily seen that if at the same A.S.I. and the same specified helix-angle in roll the altitude of the manoeuvre is increased, the tendency of the elevator load to peak is considerably aggravated. For in this case the true speed of the aeroplane is increased, as is also the actual peak rolling velocity. In particular, the pitching inertia effects are increased, and this more than anything else leads to the pull-push type of elevator co-ordination.

Thus the aim of the pilot should be so to operate the aileron that the largest rolling velocities are obtained when the angle of bank is still small.

As a corollary it may be added that since in the case of the *recovery* from a turn, the angle of bank is initially greatest, the largest rolling velocities should be delayed, so as to occur, as before, when the angle of bank is again small.

10. *The ‘Rolling Velocity’ Method.*—As a final verification of the above reasoning, a generalised ‘rolling velocity’ method is introduced, wherein considerable freedom is given to the shape of the \bar{p} vs. t curve by simple changes in parameter.

It is assumed as before that \bar{p}_{\max} and ϕ are assigned beforehand, and that the manoeuvre is completed in a finite (non-dimensional) time t_1 , to be determined. It is convenient to take new non-dimensional variables defined by

$$\begin{aligned} X &\equiv t/t_1 && (\text{so that } 0 \leq x \leq 1) \\ Y &\equiv \bar{p}/\bar{p}_{\max} && (\text{so that } 0 \leq y \leq 1) \end{aligned}$$

The general shape of curves of Y plotted against X must on geometrical and physical grounds, possess the following features (see Fig. 8a):

- (a) Be tangential to the X -axis both at the origin and at the point D (1, 0).
- (b) Have a horizontal tangent at some point B ($\lambda_2, 1$) between E and F.
- (c) Have points of inflexion at some points A (λ_1, μ_1) and C (λ_3, μ_3) between OB and BD respectively.

The points A, B, C may be said to fix the 'skeleton' of the curve, which therefore possesses five degrees of freedom corresponding to the parameters $\lambda_1, \lambda_2, \lambda_3, \mu_1$ and μ_3 . Once the 'skeleton' is chosen, the actual curve is fairly well defined because of the additional conditions of horizontal tangency at O, B and D. Hence given the 'skeleton', the complete curve may be sufficiently well represented by, for example, four individual 'parabolic' arcs OA, AB, BC, CD, each of the form

$$(Y - a_i) = k_i(X - b_i)^{m_i}, \quad (m_i > 1), \quad i = 1, 2, 3, 4.$$

Here the values of a_i, b_i and k_i are functions of the λ 's and μ 's, and are enumerated in Fig. 8a. The exponents m_i on the other hand, can be chosen arbitrarily, subject only to the condition of continuous slope at the joins A and C. However from the practical point of view it is important also that the m_i should be integers, and this places limitations on the possible positions of A and C. They are not, fortunately, severe limitations, as may be seen from Fig. 8b, which shows the loci of points A and C for convenient integral values of the m_i . In the actual numerical cases considered below, all four values of m_i will be taken equal to 2.

10.1. *The Influence of the Shape of the Rolling Velocity Curve.*—The manoeuvre considered is the former high-altitude case, retaining the same kinematical boundary conditions except for a minor change in $(pb/2U_0)_{\max}$ from 0.08984 to 0.09. The aileron and the 'dynamic' elevator loads are worked out for a range of values of the three main parameters* λ_1, λ_2 , and λ_3 .

In the case of the 'dynamic' elevator load the chief interest lies in the maximum value it attains, since reversal of control co-ordination certainly occurs whenever the 'dynamic' load exceeds the final static value to trim. The results are plotted in Fig. 9 for three broad groups corresponding to values of λ_2 of 0.2, 0.5 and 0.8 respectively. The final static load is about 8.4 lb weight, and it is seen that this is considerably exceeded by the dynamic load in all cases for which λ_2 is greater than 0.5. In fact it is only for selected cases within the group λ_2 equal to 0.2 that reversal in elevator control is avoided. This again brings out the necessity for the large rolling velocities to occur quite early on in the manoeuvre.

To complete the picture it is instructive now to examine the aileron loads which lead to the preceding co-ordinations. The values of the 'dynamic' elevator loads indicate that λ_2 may be taken as a measure of goodness of the aileron technique, which may be labelled 'Good-Fair', 'Fair-Poor' and 'Very Bad', corresponding to the values 0.2, 0.5 and 0.8 of λ_2 respectively. The resulting sets of aileron load curves are shown in Figs. 10, 11 and 12, and it is instructive to compare these with the sets of curves, Fig. 13, corresponding to the 'aileron-helix-angle' and 'synthetic' methods respectively. The 'aileron-helix-angle' method clearly bears close resemblance to the $\lambda_2 = 0.2$ 'Good-Fair' class, while the resemblance between the 'synthetic' method and the case $\lambda_2 = 0.5, \lambda_1 = 0.25, \lambda_3 = 0.7$ is even more marked, as is shown by the following tabular comparison:

Case	$\lambda_1=0.25, \lambda_2=0.5, \lambda_3=0.7$	Synthetic
Maximum aileron load	14 lb weight	13.2 lb weight
Aileron load reverses after	5.6 sec	5.5 sec
Minimum aileron load	-5.2 lb weight	-3.8 lb weight
Peak elevator load	19.3 lb weight	18 lb weight

This demonstrates the versatility of the 'rolling velocity' method, which thus by itself is capable of providing all the information of the previous methods.

* With the m_i chosen arbitrarily to have the value 2, the two conditions of continuity of slope at A and C reduce the freedom of the system nominally to three.

The classifications given above for the various types of aileron techniques lead to the following conclusion :

For good elevator co-ordination it is necessary to apply the aileron load quickly, followed by an equally rapid removal of the load. Delay in attaining peak rolling velocities is penalised by peaking elevator loads.

11. *The Manoeuvre of Recovery from Turns.*—The manoeuvre of the recovery from a turn is best regarded as a continuation of the original rolling manoeuvre into the turn. The basic condition is taken as neutral aileron angle, and the incidence and elevator settings are those appropriate to the straight flight condition. It is assumed that at the start of the manoeuvre, the above quantities differ from the basic conditions by the amounts made necessary to hold the machine into the turn. The word 'recovery' is thus used literally, in so far as the manoeuvre is the return to a basic condition from one initially displaced therefrom, rather than the departure from an original basic circling condition into a new straight line motion. It follows that the general analysis of stick loads and displacements continues to apply unchanged, the only difference in detail being the different distribution of \bar{p} and ϕ with time.

A number of examples have been worked out confirming the indications of the previous sections. Fig. 14 shows the elevator recovery loads for the two cases, 'aileron-helix-angle' method (parabolic loading), and 'synthetic' method $n = 2.9$. The order of merit of the two techniques is clearly reversed as compared with the entry into the turn. Further examples have been worked out using the 'rolling velocity' method for the cases which are expected to produce the best co-ordination. These have been taken as

$$\begin{aligned} \lambda_2 = 0.8, \quad \lambda_1 = 0.7, \quad \lambda_3 = 0.95 \\ \lambda_2 = 0.8, \quad \lambda_1 = 0.5, \quad \lambda_3 = 0.9. \end{aligned}$$

The results are shown in Fig. 15, and the improvement is most considerable. The corresponding aileron techniques have already been drawn in the previous diagram, Fig. 12.

The general conclusion is that rapid recoveries from turns at high altitudes are more difficult to perform than the entry into the turn, and that fundamentally different piloting techniques are required in accordance with the necessity, in *both* cases, of obtaining the largest rolling velocities when the angle of bank is small.

APPENDIX I

1. *Equations of Motion with Constant Forward Speed and Zero Sideslip.*—In the standard fully dimensional notation, the equations of motion of an aeroplane having constant forward speed U_0 and zero sideslip velocity are

$$m(W\dot{Q}) = X - mg \sin \theta \quad \dots \quad (1)$$

$$m(-WP + U_0R) = Y + mg \cos \theta \sin \phi \quad \dots \quad (2)$$

$$m(\dot{W} - U_0Q) = Z + mg \cos \theta \cos \phi \quad \dots \quad (3)$$

$$A\dot{P} - (B - C)QR = L \quad \dots \quad (4)$$

$$B\dot{Q} - (C - A)RP = M \quad \dots \quad (5)$$

$$C\dot{R} - (A - B)PQ = N \quad \dots \quad (6)$$

where

$$P = \dot{\phi} - \dot{\psi} \sin \theta \quad \dots \quad (7)$$

$$Q = \dot{\theta} \cos \phi + \dot{\psi} \cos \theta \sin \phi \quad \dots \quad (8)$$

$$R = -\dot{\theta} \sin \phi + \dot{\psi} \cos \theta \cos \phi \quad \dots \quad (9)$$

Let T^* be the airscrew thrust assumed acting along the X -axis, and let α_0 and T_0^* represent the incidence and thrust acting in the steady horizontal flight condition immediately prior to the manoeuvre. The initial steady conditions are

$$Y_0 = L_0 = M_0 = N_0 = P_0 = Q_0 = R_0 = \theta_0 = \phi_0 = 0$$

while also W_0 is zero if wind axes are used. Equations (1) and (3) reduce to

$$X_0 = 0 = T_0^* - \frac{1}{2}\rho S U_0^2 C_D(\alpha_0) \quad \dots \quad (10)$$

and

$$Z_0 + mg = 0 \quad \dots \quad (11)$$

Assume that during the course of the manoeuvre, terms like Z and L take values given by

$$Z = Z_0 + Z_q Q + Z_w W + Z_\eta \eta$$

$$L = L_0 + L_p P + L_r R + L_\xi \xi$$

and that in these expressions the derivatives are functions of the actual incidence appertaining at any instant. The equations of motion may thus be written

$$m(W\dot{Q}) - X_w W - X_q Q + mg \sin \theta = T^* - T_0^* \quad \dots \quad (12)$$

$$m(-WP + U_0R - g \cos \theta \sin \phi) = Y_\xi \xi \quad \dots \quad (13)$$

$$m(\dot{W} - U_0Q - g \cos \theta \cos \phi) - Z_0 - Z_q Q - Z_w W = Z_\eta \eta \quad \dots \quad (14)$$

$$A\dot{P} - (B - C)QR - L_p P - L_r R = L_\xi \xi \quad \dots \quad (15)$$

$$B\dot{Q} - (C - A)RP - M_w W - M_q Q = M_\eta \eta \quad \dots \quad (16)$$

$$C\dot{R} - (A - B)PQ - N_p P - N_r R = N_\xi \xi \quad \dots \quad (17)$$

while equations (7), (8) and (9) remain as before.

2. *The Non-Dimensional Form of the Equations.*—It is convenient to denote the non-dimensional form of any variable by the same symbol in small type* with a bar above. An exception is made in the case of the non-dimensional symbol for time, from which the bar is

* Symbols in small type, e.g., \bar{p} , \bar{w} , are generally taken to mean the small, dimensional increases from the steady values of the variables P , W . The bar is here the distinguishing feature of non-dimensionality.

omitted. Thus T denoting time in seconds, and τ the unit of time defined by $\tau = m/\rho S U_0$, the non-dimensional time t is given by the relation

$$T = t\tau.$$

Taking, now the semi-span s as the unit of length, the scheme of non-dimensionalisation is as shown below, it being understood that an expression like \dot{w} means dW/dT whereas $\dot{\bar{w}}$ means $d\bar{w}/dt$.

Write

$$\begin{aligned} W &= \bar{w}(s/\tau), \text{ etc., for linear velocities} \\ \dot{W} &= \dot{\bar{w}}(s/\tau^2), \text{ etc., for linear accelerations} \\ P &= \bar{p}(1/\tau), \text{ etc., for angular velocities} \\ \dot{P} &= \dot{\bar{p}}(1/\tau^2), \text{ etc., for angular accelerations} \\ X_w &= x_w(m/\tau), \text{ etc., for force-velocity derivatives} \\ Z_q &= z_q(ms/\tau), \text{ etc., for force-angular-velocity derivatives} \\ M_w &= m_w(ms/\tau), \text{ etc., for moment-velocity derivatives} \\ M_{\dot{w}} &= m_{\dot{w}}(ms), \text{ etc., for moment-acceleration derivatives} \\ L_p &= l_p(ms^2/\tau), \text{ etc., for moment-angular-velocity derivatives} \\ Y_{\zeta} &= y_{\zeta}(mU_0/\tau), \text{ etc., for force-control-angle derivatives} \\ M_{\eta} &= m_{\eta}(mU_0s/\tau), \text{ etc., for moment-control-angle derivatives} \\ X &= \frac{1}{2}\rho S U_0^2 C_x \text{ for forces} \\ L &= \frac{1}{2}\rho S U_0^2 b C_l \text{ for lateral moments } (b = 2s) \\ M &= \frac{1}{2}\rho S U_0^2 c C_m \text{ for longitudinal moments } (c = \text{wing chord}) \\ X_0 &= x_0(ms/\tau^2), \text{ etc., for initial forces} \\ A &= ms^2 i_A, \text{ etc., for lateral moments of inertia} \\ B &= ms^2 i_B \text{ for the longitudinal moment of inertia} \\ \mu &= m/\rho S s = U_0\tau/s, \text{ the height parameter} \\ \mu\bar{k} &= \tau^2 g/s, \text{ definition of } \bar{k}. \end{aligned}$$

This differs somewhat from the normal longitudinal procedure because of the use of the semi-span s for the unit of length. The expressions which occur in the equations of motion, however, do not ultimately depend on the choice of length unit, since fundamental terms like $\mu m_w/i_B$, l_p/i_A , etc., are equivalent to $M_w \tau^2 U_0/B$, $L_p \tau/A$ respectively, and these are fixed measurable physical quantities.

Substituting the above expressions in the equations of motion, and denoting expressions like $i_B - i_C$ by \bar{A} and neglecting Z_q , X_q , X_r which are small, the equations take the form

$$\bar{w}\bar{q} - x_w\bar{w} + \mu\bar{k} \sin \theta = (T^* - T_0^*)(\tau^2/ms) \dots \dots (18)$$

$$-\bar{w}\bar{p} + \mu\bar{r} - \mu\bar{k} \cos \theta \sin \phi = \mu y_{\zeta} \zeta \dots \dots (19)$$

$$\dot{\bar{w}} - \mu\bar{q} - z_w\bar{w} - z_0 - \mu\bar{k} \cos \theta \cos \phi = \mu z_{\eta} \eta \dots \dots (20)$$

$$i_A \dot{\bar{p}} - \bar{A} \bar{q}\bar{r} - l_p \bar{p} - l_r \bar{r} = \mu l_{\zeta} \zeta \dots \dots (21)$$

$$i_B \dot{\bar{q}} - \bar{B} \bar{r}\bar{p} - m_w \bar{w} - m_{\dot{w}} \dot{\bar{w}} - m_q \bar{q} = \mu m_{\eta} \eta \dots \dots (22)$$

$$i_C \dot{\bar{r}} - \bar{C} \bar{p}\bar{q} - n_p \bar{p} - n_r \bar{r} = \mu n_{\zeta} \zeta + \mu n_{\xi} \xi \dots \dots (23)$$

together with the relations

$$\bar{p} = \dot{\phi} - \dot{\psi} \sin \theta \quad \dots \quad (24)$$

$$\bar{q} = \dot{\theta} \cos \phi + \dot{\psi} \cos \theta \sin \phi \quad \dots \quad (25)$$

$$\bar{r} = -\dot{\theta} \sin \phi + \dot{\psi} \cos \theta \cos \phi \quad \dots \quad (26)$$

In addition there is the condition for no loss of height during the manoeuvre, namely

$$U_0 \sin \theta = W \cos \theta \cos \phi$$

whence $\tan \theta = \frac{\bar{w}}{\mu} \cos \phi \quad \dots \quad (27)$

3. *Solution of Equations of Motion in Terms of \bar{p} and ϕ .*—(a) *Preliminary Relations.*—The increase in incidence from the original straight flight condition is W/U_0 or \bar{w}/μ . Since this is not likely to be more than about 12 deg, we may from equation (27) replace $\tan \theta$ by θ . This same equation on differentiation gives

$$\dot{\theta} = \frac{\dot{\bar{w}}}{\mu} \cos \phi - \frac{\bar{w}}{\mu} \sin \phi \dot{\phi} \quad \dots \quad (28)$$

Consider now the relation between \bar{k} , C_L and z_0 .

By definition of section 2,

$$\bar{k} = \frac{\tau^2 g}{\mu S} = \frac{\tau g}{U_0} = \frac{mg}{\rho S U_0^2}$$

Hence $\bar{k} = \frac{1}{2} C_L(\alpha_0) \quad \dots \quad (29)$

Again,

$$z_0 = \frac{\tau^2}{mS} Z_0$$

Hence by (11),

$$z_0 = \frac{\tau^2}{mS} (-mg) = -\frac{\tau^2 g}{S} = -\mu \bar{k} \quad \dots \quad (30)$$

(b) *Solution of Equations for \bar{w} .*—Equation (20) may be written by virtue of (30)

$$\dot{\bar{w}} - z_w \bar{w} = \mu [\bar{q} + \bar{k}(\cos \theta \cos \phi - 1) + z_w \eta] \quad \dots \quad (31)$$

Now from (25) and (26)

$$\bar{q} = \bar{r} \tan \phi + \dot{\theta} \sec \phi \quad \dots \quad (32)$$

or from (19) and (28)

$$\bar{q} = \left(\frac{\bar{w}}{\mu} \bar{p} + \bar{k} \cos \theta \sin \phi + y_\zeta \zeta \right) \tan \phi + \left(\frac{\dot{\bar{w}}}{\mu} - \frac{\bar{w}}{\mu} \tan \phi \dot{\phi} \right)$$

i.e.,

$$\bar{q} = \frac{\dot{\bar{w}}}{\mu} + \frac{\bar{w}}{\mu} \tan \phi (\bar{p} - \dot{\phi}) + \bar{k} \cos \theta \frac{\sin^2 \phi}{\cos \phi} + y_\zeta \zeta \tan \phi$$

Substituting in (31), we get

$$\frac{\dot{\bar{w}}}{\mu} - z_w \frac{\bar{w}}{\mu} = \frac{\dot{\bar{w}}}{\mu} + \frac{\bar{w}}{\mu} \tan \phi (\bar{p} - \dot{\phi}) + \bar{k} \cos \theta \left(\cos \phi + \frac{\sin^2 \phi}{\cos \phi} - \sec \theta \right) + z_w \eta + y_\zeta \zeta \tan \phi$$

Hence from (24), substituting for \bar{p} ,

$$-z_w \frac{\bar{w}}{\mu} = -\frac{\bar{w}}{\mu} \tan \phi \sin \theta \dot{\psi} + \bar{k}(\cos \theta \sec \phi - 1) + z_w \eta + y_\zeta \zeta \tan \phi$$

In the expression on the right-hand side we assume that only the term in \bar{k} is of importance. This is not quite obvious in the very initial stages of the motion, but we can say that the first term is of the fourth order in small quantities, and that the effect of neglecting $z_\eta \eta$ and $y_\zeta \zeta \tan \phi$ may be assessed *a posteriori* from the values of η and ζ later to be calculated. The equation therefore reduces to

$$\frac{\bar{w}}{\mu} = \Delta\alpha = -\frac{\bar{k}}{z_w} (\cos \theta \sec \phi - 1).$$

But

$$z_w \approx -\frac{1}{2} \frac{dC_L}{d\alpha} = -\frac{\bar{k}}{\alpha_0},$$

hence

$$\frac{\bar{w}}{\mu} = \Delta\alpha = \alpha_0 (\cos \theta \sec \phi - 1). \quad \dots \quad \dots \quad \dots \quad \dots \quad \dots \quad \dots \quad \dots \quad \dots \quad \dots \quad (33)$$

As a check on the size of θ , (27) yields

$$\tan \theta = \alpha_0 (\cos \theta \sec \phi - 1) \cos \phi.$$

Let N denote the additional load factor in the manoeuvre. Then

$$N = \frac{\bar{w}/\mu}{\alpha_0} = \cos \theta \sec \phi - 1.$$

Therefore $\tan \theta = \alpha_0 N \cos \phi = \alpha_0 N \frac{\cos \theta}{N + 1}$

i.e., $\sin \theta = \frac{\alpha_0 N}{N + 1} \cos^2 \theta.$

Now the total incidence is $\alpha_0(N + 1)$ and cannot exceed about 0.3 radians or else the aircraft will stall. Hence $\alpha_0(N + 1) = 0.3 - \varepsilon$ where $\varepsilon > 0$, while

$$\sin \theta = \frac{(0.3 - \varepsilon - \alpha_0)\alpha_0}{(0.3 - \varepsilon)} \cos^2 \theta.$$

The maximum value of this occurs when $\alpha_0 = \frac{1}{2}(0.3 - \varepsilon)$, giving

$$(\sin \theta)_{\max} < \frac{(0.3 - \varepsilon)}{4} < 0.075.$$

Hence

$$\theta < 4.3 \text{ deg.}$$

and

$$(\cos \theta)_{\min} > 0.9972.$$

We are therefore justified in replacing $\sin \theta$ by θ and $\cos \theta$ by unity wherever it occurs. In particular, equation (24) gives

$$\bar{p} = \dot{\bar{\phi}} \quad \dots \quad \dots \quad \dots \quad \dots \quad \dots \quad \dots \quad \dots \quad \dots \quad \dots \quad (34)$$

while (33) above reduces to

$$\frac{\bar{w}}{\mu} = \Delta\alpha = \alpha_0 (\sec \phi - 1). \quad \dots \quad \dots \quad \dots \quad \dots \quad \dots \quad \dots \quad \dots \quad \dots \quad \dots \quad (35)$$

(c) *Solution for \bar{q} .*—We have previously obtained the relation

$$\bar{q} = \frac{\dot{w}}{\mu} + \frac{\bar{w}}{\mu} \tan \phi (\bar{p} - \dot{\bar{\phi}}) + \bar{k} \cos \theta \frac{\sin^2 \phi}{\cos \phi} + y_\zeta \zeta \tan \phi.$$

Neglecting the y_t term, and using the results of (34) and (35), which yield

$$\frac{\dot{\bar{w}}}{\mu} = \alpha_0 \sec \phi \tan \phi \bar{p} \quad \dots \quad \dots \quad \dots \quad \dots \quad \dots \quad \dots \quad \dots \quad (36)$$

we get

$$\bar{q} = \alpha_0 \sec \phi \tan \phi \bar{p} + \bar{k} \sin^2 \phi \sec \phi .$$

Define $a \equiv dC_L/d\alpha$. Then

$$\bar{q} = \frac{1}{2}C_L(\alpha_0) \left[(\sec \phi - \cos \phi) + \sec \phi \tan \phi \frac{2}{a} \bar{p} \right] \quad \dots \quad \dots \quad \dots \quad (37)$$

(d) *Solution for \bar{r} .*—Equation (19) yields on neglecting y_t

$$\bar{r} = \bar{k} \sin \phi + \frac{\bar{w}}{\mu} \bar{p}$$

whence from equation (35)

$$\bar{r} = \frac{1}{2}C_L(\alpha_0) \left[(\sin \phi) + (\sec \phi - 1) \frac{2}{a} \bar{p} \right] . \quad \dots \quad \dots \quad \dots \quad \dots \quad (38)$$

(e) *Solution for $\dot{\bar{\psi}}$.*—Equation (26) may be written

$$\dot{\bar{\psi}} = \bar{r} \sec \phi + \bar{\theta} \tan \phi .$$

But from (28), (35) and (36)

$$\bar{\theta} = (\alpha_0 \sec \phi \tan \phi \bar{p}) \cos \phi - \alpha_0 (\sec \phi - 1) \sin \phi \bar{p}$$

or

$$\bar{\theta} = \alpha_0 \bar{p} \sin \phi (\sec \phi - \sec \phi + 1) = \alpha_0 \bar{p} \sin \phi .$$

Therefore

$$\dot{\bar{\psi}} = \frac{1}{2}C_L(\alpha_0) \left[(\tan \phi) + (\sec^2 \phi - \sec \phi + \sin^2 \phi \sec \phi) \frac{2}{a} \bar{p} \right] ,$$

therefore

$$\dot{\bar{\psi}} = \frac{1}{2}C_L(\alpha_0) \left[(\tan \phi) + (\sec^2 \phi - \cos \phi) \frac{2}{a} \bar{p} \right] . \quad \dots \quad \dots \quad \dots \quad \dots \quad (39)$$

It is helpful at this stage to recall the assumptions adopted: that the direct effects of the forces produced by the controls are small, and that the controls primarily serve to produce moments about the c.g. On this understanding, equation (19), which so far has not been used, tells us how the thrust must be adjusted to satisfy the requirement of constancy of speed.

4. *Basic ϕ Functions.*—In the general case the values of \bar{p} and ϕ will be known as functions of time, either directly as in the 'synthetic' method, or as the result of the solution of the rolling equation, as in the 'aileron' methods. The values of ξ , η and ζ may therefore be found as functions of time from equations (21), (22) and (23).

To facilitate the calculation of the control deflections and loads, we introduce new symbols as follows:

$$q_1 \equiv (\sec \phi - \cos \phi) \quad \dots \quad \dots \quad \dots \quad \dots \quad \dots \quad \dots \quad \dots \quad (40)$$

$$q_2 \equiv \sec \phi \tan \phi \quad \dots \quad \dots \quad \dots \quad \dots \quad \dots \quad \dots \quad \dots \quad (41)$$

$$r_1 \equiv \sin \phi \quad \dots \quad \dots \quad \dots \quad \dots \quad \dots \quad \dots \quad \dots \quad (42)$$

$$r_2 \equiv (\sec \phi - 1) \quad \dots \quad \dots \quad \dots \quad \dots \quad \dots \quad \dots \quad \dots \quad (43)$$

$$\dot{\bar{\psi}}_1 \equiv \tan \phi \quad \dots \quad \dots \quad \dots \quad \dots \quad \dots \quad \dots \quad \dots \quad (44)$$

$$\bar{\psi}_2 \equiv \sec^2 \phi - \cos \phi . \quad \dots \quad \dots \quad \dots \quad \dots \quad \dots \quad \dots \quad \dots \quad (45)$$

Then
$$\bar{q} = \frac{1}{2}C_L\left(q_1 + q_2 \frac{2\bar{p}}{a}\right) \quad \dots \quad \dots \quad \dots \quad \dots \quad \dots \quad \dots \quad \dots \quad (46)$$

$$\bar{r} = \frac{1}{2}C_L\left(r_1 + r_2 \frac{2\bar{p}}{a}\right) \quad \dots \quad \dots \quad \dots \quad \dots \quad \dots \quad \dots \quad \dots \quad (47)$$

$$\dot{\bar{p}} = \frac{1}{2}C_L\left(\dot{\bar{p}}_1 + \dot{\bar{p}}_2 \frac{2\bar{p}}{a}\right) \quad \dots \quad \dots \quad \dots \quad \dots \quad \dots \quad \dots \quad \dots \quad (48)$$

while

$$\frac{\dot{\bar{w}}}{\mu} = \frac{1}{a} C_L r_2 \dots \quad \dots \quad \dots \quad \dots \quad \dots \quad \dots \quad \dots \quad \dots \quad (49)$$

We also require expressions for $\dot{\bar{q}}$, $\dot{\bar{r}}$ and $\dot{\bar{w}}/\mu$.

Writing
$$\frac{d}{dt} = \frac{d}{d\phi} \frac{d\phi}{dt} = \bar{p} \frac{d}{d\phi}$$

we get
$$\dot{\bar{q}} = \frac{1}{2}C_L \left[\bar{p} \left(\frac{dq_1}{d\phi} + \frac{2\bar{p}}{a} \frac{dq_2}{d\phi} \right) + q_2 \frac{2}{a} \dot{\bar{p}} \right] \quad \dots \quad \dots \quad \dots \quad \dots \quad \dots \quad (50)$$

$$\dot{\bar{r}} = \frac{1}{2}C_L \left[\bar{p} \left(\frac{dr_1}{d\phi} + \frac{2\bar{p}}{a} \frac{dr_2}{d\phi} \right) + r_2 \frac{2}{a} \dot{\bar{p}} \right] \quad \dots \quad \dots \quad \dots \quad \dots \quad \dots \quad (51)$$

and

$$\frac{\dot{\bar{w}}}{\mu} = \frac{1}{a} C_L \left(\bar{p} \frac{dr_2}{d\phi} \right) = \frac{1}{2}C_L \left(\frac{2\bar{p}}{a} \frac{dr_2}{d\phi} \right) \dots \quad \dots \quad \dots \quad \dots \quad \dots \quad (52)$$

The values of the differentials with respect of ϕ are

$$\frac{dq_1}{d\phi} = \sec \phi \tan \phi + \sin \phi \quad \dots \quad \dots \quad \dots \quad \dots \quad \dots \quad \dots \quad \dots \quad (53)$$

$$\frac{dq_2}{d\phi} = \sec \phi (\tan^2 \phi + \sec^2 \phi) = \sec \phi (1 + 2 \tan^2 \phi) \quad \dots \quad \dots \quad \dots \quad (54)$$

$$\frac{dr_1}{d\phi} = \cos \phi \quad \dots \quad \dots \quad \dots \quad \dots \quad \dots \quad \dots \quad \dots \quad (55)$$

$$\frac{dr_2}{d\phi} = \sec \phi \tan \phi = q_2 \dots \quad \dots \quad \dots \quad \dots \quad \dots \quad \dots \quad \dots \quad (56)$$

In practice it is helpful to plot graphs of the more important of the above quantities on a very open scale with ϕ as abscissa, taking 1 cm for each degree of ϕ . The functions q_1 and r_2 are most conveniently plotted together, as are also q_2 and $dq_1/d\phi$, but $dq_2/d\phi$ is plotted by itself. Each of these three sets of curves occupies four sheets of quarto size graph paper, and the ordinates are limited to the range zero to unity by the device of plotting the reciprocals of the functions whenever unity is exceeded. In this way the quantities, in the important range of ϕ , may always be read to three, and sometimes four significant figures.

The advantage of having these ready plotted curves is very great, since \bar{q} , $\dot{\bar{q}}$, etc., may be evaluated with extreme ease, seeing that \bar{p} and ϕ are presumed known. It is more convenient, however, to derive explicit expressions for ξ , η and ζ in terms of \bar{p} and ϕ and the derivatives.

We remember in this case that since n_p and l_r are linear functions of incidence, their values at any instant are

$$n_p \frac{\alpha_0 + \Delta\alpha}{\alpha_0} \text{ and } l_r \frac{\alpha_0 + \Delta\alpha}{\alpha_0},$$

i.e.,

$$n_p \sec \phi \text{ and } l_r \sec \phi.$$

The actual values of ξ , η and ζ are calculated from equations (21), (22) and (23). In these we may neglect the terms in \bar{A} , \bar{B} , \bar{C} without much loss in accuracy. The values thus become

$$\frac{\mu l_\xi \dot{\xi}(t)}{i_A} = \dot{\bar{p}} - \bar{p} \left[\frac{l\dot{\phi}}{i_A} + \frac{C_L l_r}{a i_A} (r_2 \sec \phi) \right] - \frac{1}{2} C_L \frac{l_r}{i_A} (r_1 \sec \phi) \quad \dots \quad \dots \quad \dots \quad (57)$$

$$\begin{aligned} \frac{\mu m_\eta \dot{\eta}(t)}{i_B} = & \frac{1}{2} C_L \left\{ \frac{2q_2}{a} \dot{\bar{p}} + \bar{p} \left[\frac{dq_1}{d\phi} + \frac{2\bar{p}}{a} \frac{dq_2}{d\phi} - \frac{2q_2}{a} \left(\frac{\mu m_w}{i_B} + \frac{m_q}{i_B} \right) \right] \right. \\ & \left. - \left(\frac{\mu m_w}{i_B} \frac{2r_2}{a} + \frac{m_q}{i_B} q_1 \right) \right\} \quad \dots \quad \dots \quad \dots \quad \dots \quad \dots \quad \dots \quad (58) \end{aligned}$$

and

$$\begin{aligned} \frac{\mu n_\zeta \dot{\zeta}(t)}{i_C} = & \frac{1}{2} C_L \left\{ \frac{2r_2}{a} \dot{\bar{p}} + \bar{p} \left[\frac{dr_1}{d\phi} + \frac{2\bar{p}}{a} \frac{dr_2}{d\phi} - \frac{2}{i_C} \left(\frac{n_p \sec \phi}{C_L} + \frac{n_r r_2}{a} \right) \right] \right. \\ & \left. - \left(\frac{n_r}{i_C} r_1 + \frac{\mu n_\xi}{i_C} \xi(t) \frac{2}{C_L} \right) \right\} \quad \dots \quad \dots \quad \dots \quad \dots \quad \dots \quad \dots \quad (59) \end{aligned}$$

This is a complete statement of the problem as far as control deflections are concerned.

APPENDIX II

The 'Aileron-Helix-Angle' Method (a)—Triangular Loading

1. Let us assume that the aileron load is always applied linearly in the manner of the diagram, the rate of application being the same as the rate of reduction of load, each period taking t_1 units of time.

We shall show that a maximum value of $(pb/2U_0)$ is attained between A and B and we shall further deduce rules for solving the kinematics of the motion completely when both $(pb/2U_0)_{\max}$ and ϕ_∞ are assigned.

2. *Theory.*—We write the equation for rolling in the general form

$$\dot{\bar{p}} + h'\bar{p} = F_i + G_i t \quad \dots \quad (1)$$

where suffix i applies to individual linear sections of the aileron load curve,

$$h' \equiv -\frac{l_p}{i_A} \left(1 + \frac{l_\xi b_1}{l_p b_2} \right)$$

and

$$F_i + G_i t = \frac{\mu l_\xi (C_H)}{i_A 2b_2} \quad \dots \quad (2)$$

For Stage OA ,

$$F_1 = 0, \quad G_1 t_1 = (C_H)_{\max} \frac{\mu l_\xi}{i_A 2b_2} \quad \dots \quad (3)$$

The solution for \bar{p} is

$$\bar{p} = \frac{G_1 t}{h'} - \frac{G_1}{(h')^2} (1 - e^{-h' t}) \quad \dots \quad (4)$$

whence the rolling velocity at A is given by

$$\bar{p}_1 = \frac{G_1 t_1}{h'} - \frac{G_1}{(h')^2} (1 - e^{-h' t_1}) \quad \dots \quad (5)$$

From (4)

$$\dot{\bar{p}} = \frac{G_1}{h'} - \frac{G_1}{(h')} \cdot e^{-h' t} = \frac{G_1}{h'} (1 - e^{-h' t}) > 0.$$

Hence \bar{p} increases steadily between O and A .

For Stage AB ,

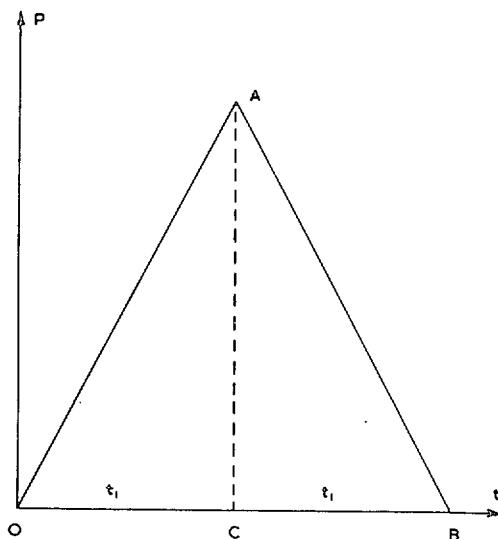
$$\dot{\bar{p}} + h'\bar{p} = G_1(t_1 - t) \quad \dots \quad (6)$$

Here

$$\begin{aligned} F_2 &= G_1 t_1 \\ G_2 &= -G_1. \end{aligned}$$

The solution of (6) with initial condition $\bar{p} = \bar{p}_1$ is

$$\bar{p} = \bar{p}_1 e^{-h' t} - \frac{G_1 t}{h'} + \frac{1}{(h')^2} [G_1 t_1 h' + G_1] (1 - e^{-h' t}).$$



Hence from (5)

$$\bar{p} = \left[\frac{G_1 t_1}{h'} - \frac{G_1}{(h')^2} (1 - e^{-h' t_1}) \right] e^{-h' t} - \frac{G_1 t}{h'} + \frac{G_1}{(h')^2} (1 + h' t_1) (1 - e^{-h' t}).$$

When \bar{p} is a maximum $d\bar{p}/dt = 0$. This occurs when

$$0 = \frac{G_1}{h'} \left[t_1 - \frac{(1 - e^{-h' t_1})}{h'} \right] (-h' e^{-h' t}) - \frac{G_1}{h'} + \frac{G_1}{h'} (1 + h' t_1) e^{-h' t}$$

or

$$0 = e^{-h' t} [-h' t_1 + (1 - e^{-h' t_1}) + (1 + h' t_1)] - 1$$

i.e.,

$$e^{-h' t} = \frac{1}{2 - e^{-h' t_1}} \quad \dots \quad \dots \quad \dots \quad \dots \quad \dots \quad \dots \quad \dots \quad \dots \quad \dots \quad (7)$$

Let the solution of (7) be $t = \bar{t}$.

Then from (6)

$$\bar{p}_{\max} = \frac{G_1(t_1 - \bar{t})}{h'} \quad \left. \begin{array}{l} \dots \dots \dots \dots \dots \dots \\ \dots \dots \dots \dots \dots \dots \end{array} \right\} \quad \dots \quad \dots \quad \dots \quad \dots \quad \dots \quad \dots \quad \dots \quad (8)$$

where

$$\bar{t} = \frac{1}{h'} \cdot \log_e (2 - e^{-h' t_1}). \quad \left. \begin{array}{l} \dots \dots \dots \dots \dots \dots \\ \dots \dots \dots \dots \dots \dots \end{array} \right\} \quad \dots \quad \dots \quad \dots \quad \dots \quad \dots \quad \dots \quad \dots \quad (9)$$

We have to verify in this that $t_1 > \bar{t}$ since equation (6) only holds for $t_1 > t$.

We require $t_1 > \frac{1}{h'} \log_e (2 - e^{-h' t_1})$.

Writing $h' t_1 = X$ we have to show that

$$X > \log_e (2 - e^{-X}),$$

i.e., that

$$e^X > 2 - e^{-X}$$

or that

$$\cosh X > 1.$$

The condition is therefore satisfied, and the peak value of \bar{p} necessarily occurs between A and B.

We have so far determined \bar{p}_{\max} , in terms explicitly of the quantity G_1 and implicitly of t_1 . We have yet to introduce the known value of ϕ_∞ .

Integrate equation (1) between limits of t of 0 and infinity. The left-hand side becomes simply $h' \phi_\infty$, while the right-hand side represents the area of triangle OAB, i.e., $G_1 t_1^2$.

Hence

$$G_1 t_1 = \frac{h' \phi_\infty}{t_1} \quad \dots \quad \dots \quad \dots \quad \dots \quad \dots \quad \dots \quad \dots \quad \dots \quad \dots \quad (10)$$

Substituting in equation (8), we get with the aid of (9).

$$\bar{p}_{\max} = \frac{\phi_\infty}{t_1} - \frac{G_1}{(h')^2} \log_e (2 - e^{-h' t_1}),$$

therefore

$$\bar{p}_{\max} = \frac{\phi_\infty}{t_1} - \frac{\phi_\infty}{h' (t_1)^2} \log_e (2 - e^{-h' t_1}).$$

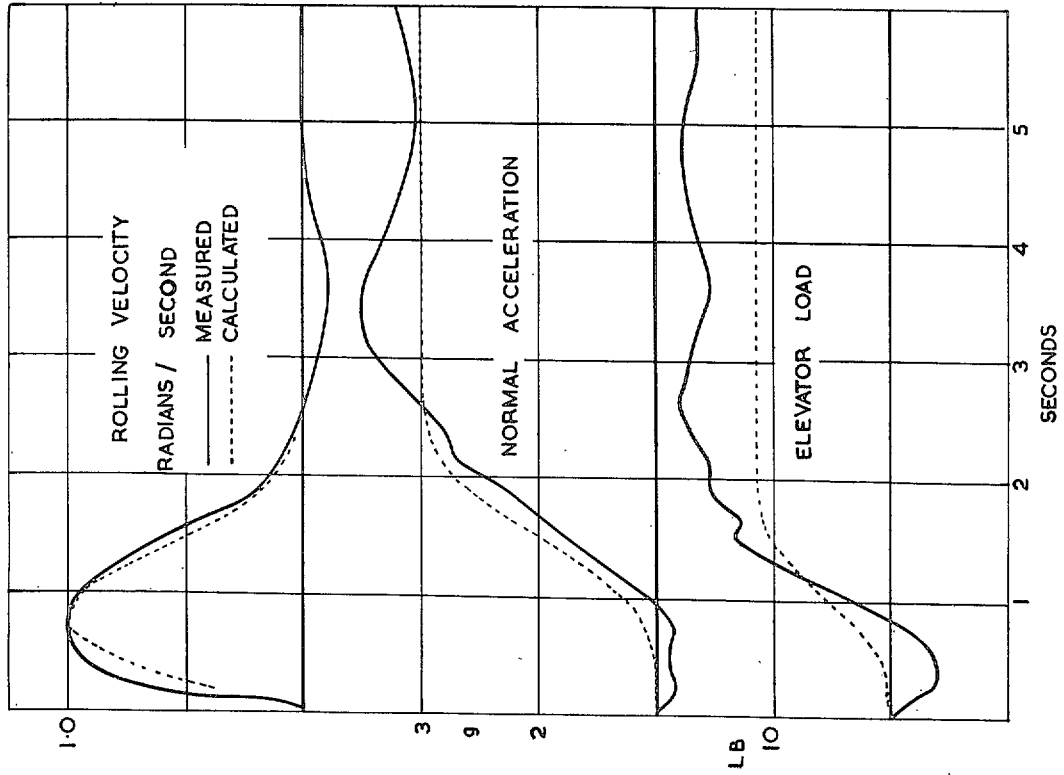


FIG. 1.

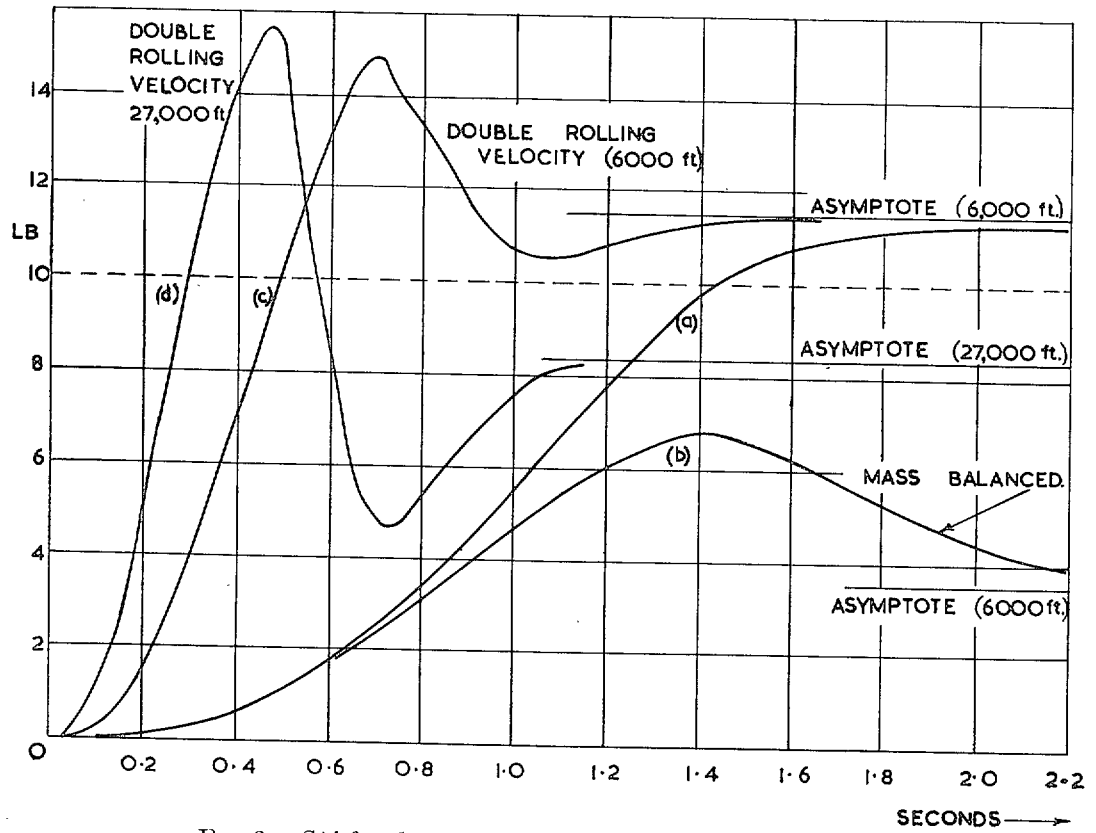


FIG. 2. *Spitfire* elevator loads. 3g turn at 250 m.p.h. A.S.I.

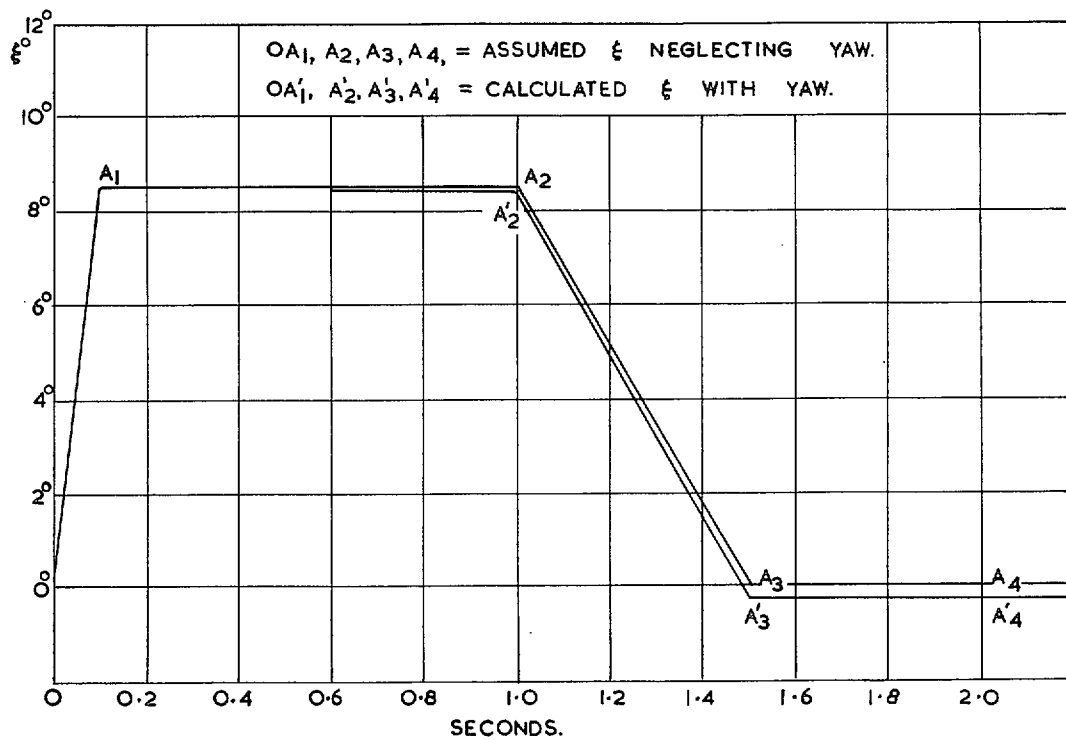


FIG. 3. Aileron deflection. 3g turn at 228.7 m.p.h. A.S.T.

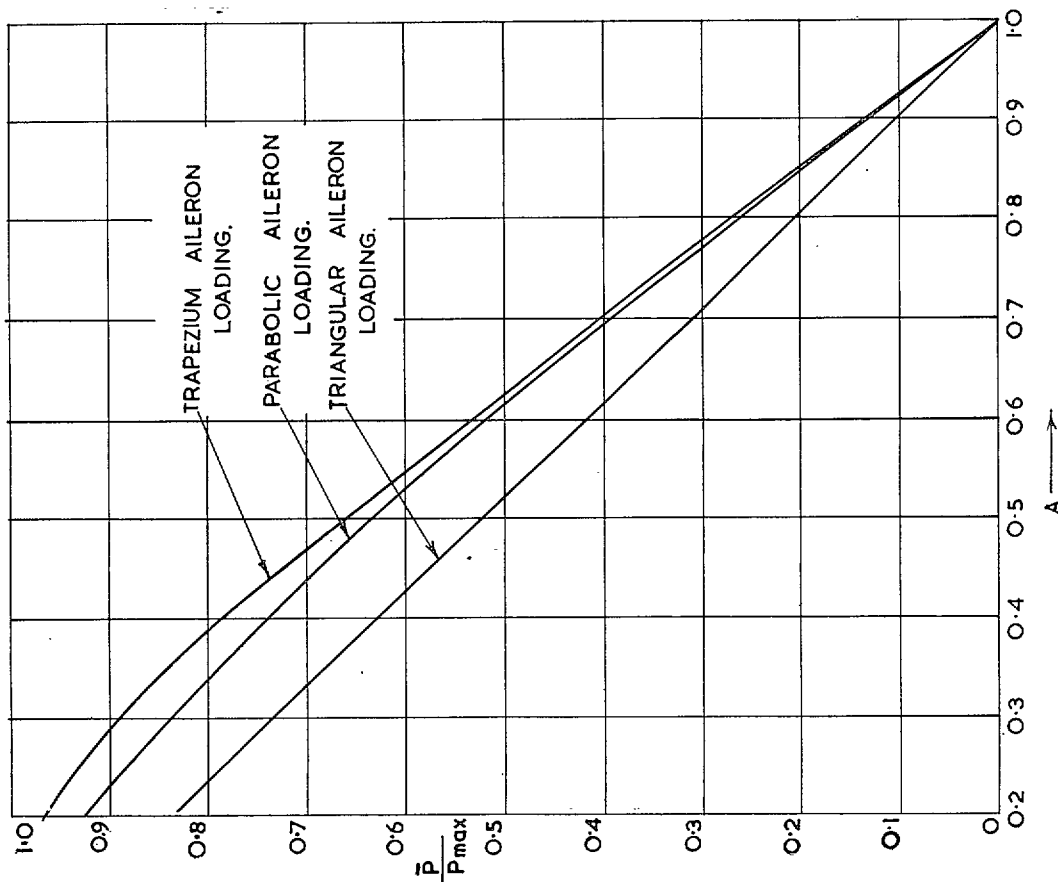


FIG. 4. Comparison of different piloting techniques.

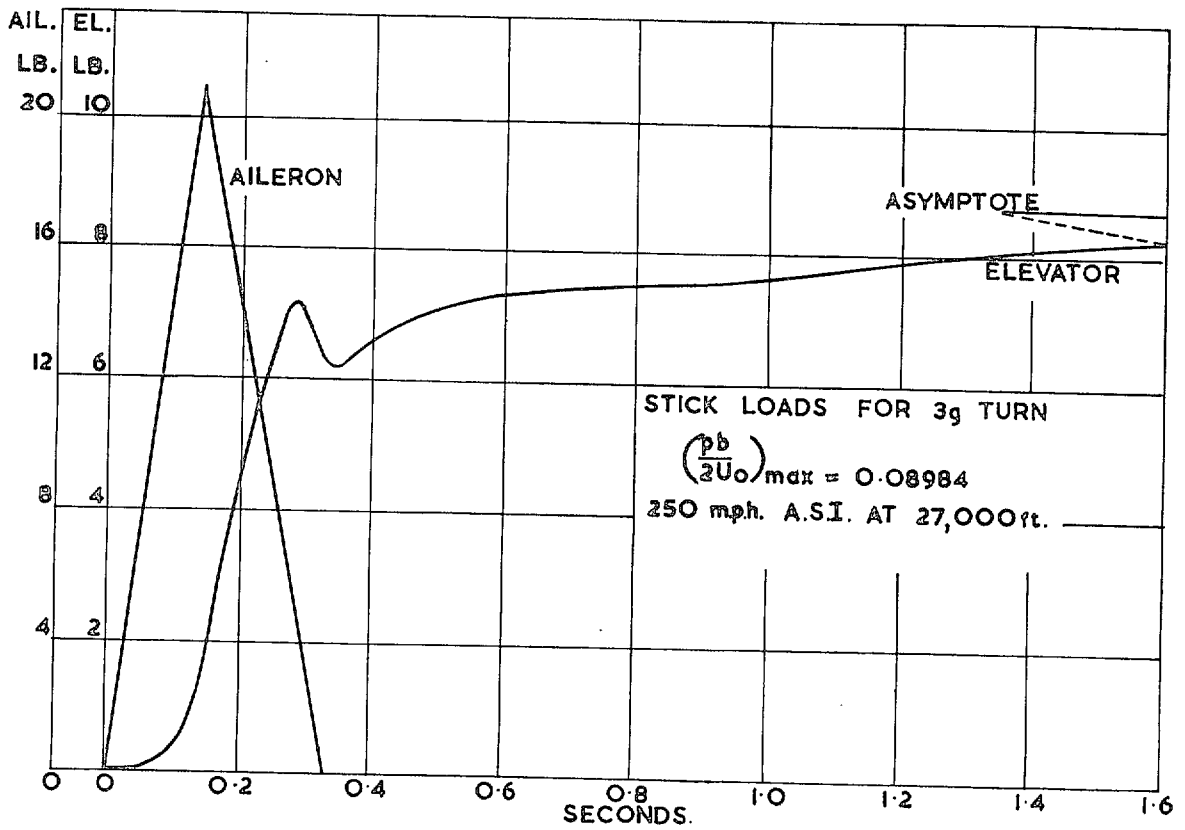


FIG. 5. Triangular aileron loading.

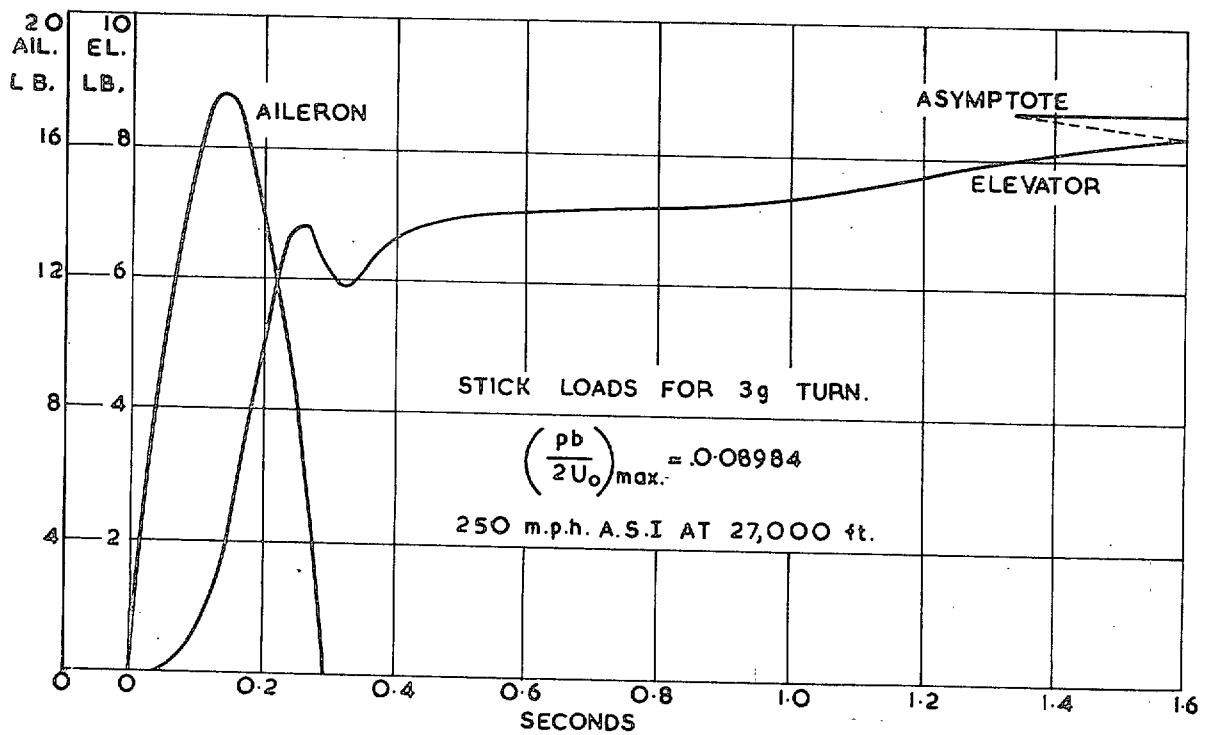


FIG. 6. Parabolic aileron loading.

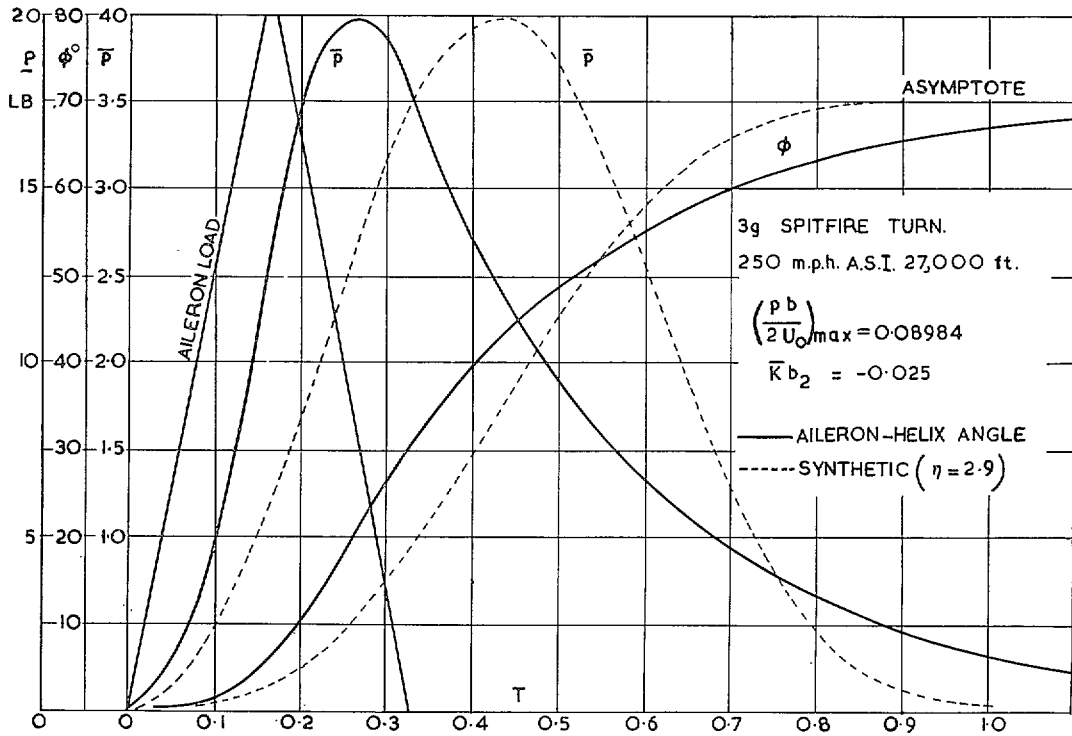


FIG. 7.

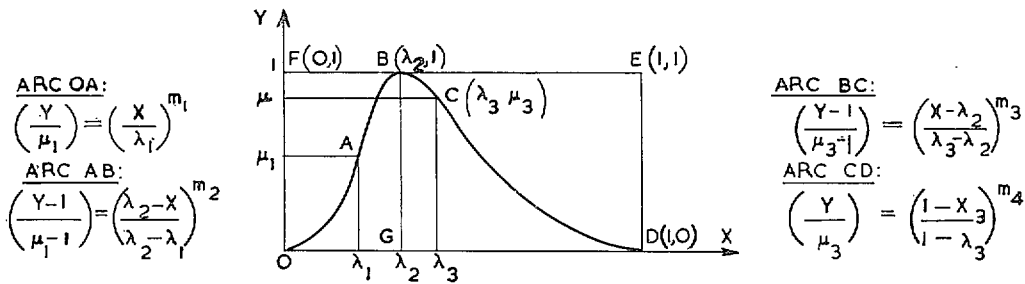


FIG. 8a. Typical X vs. Y curve.

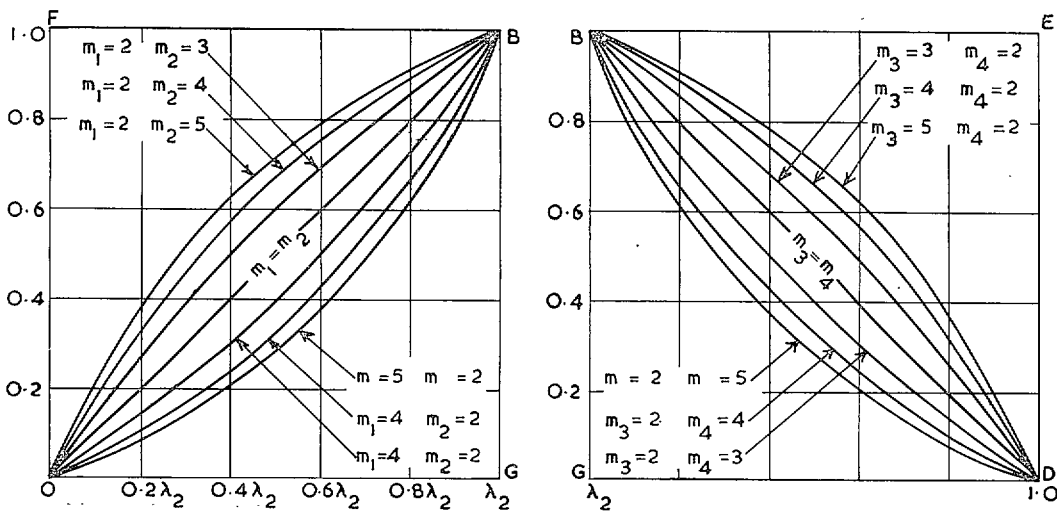


FIG. 8b.

Locus of point A for given parabolic-arcs.

Locus of point C for given parabolic-arcs.

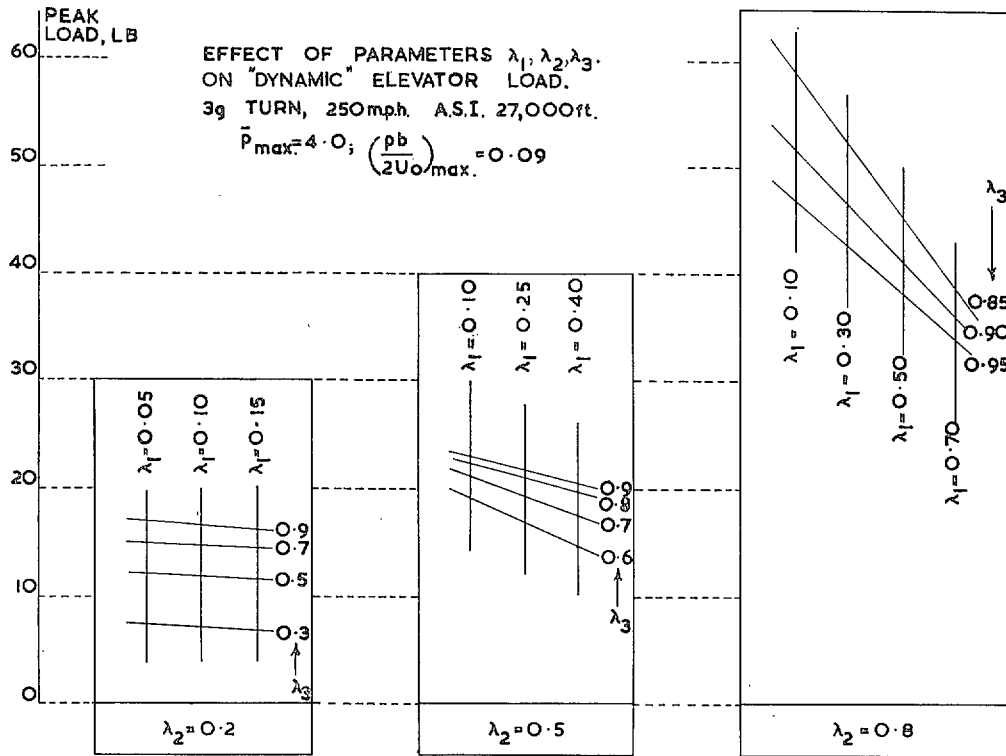


FIG. 9

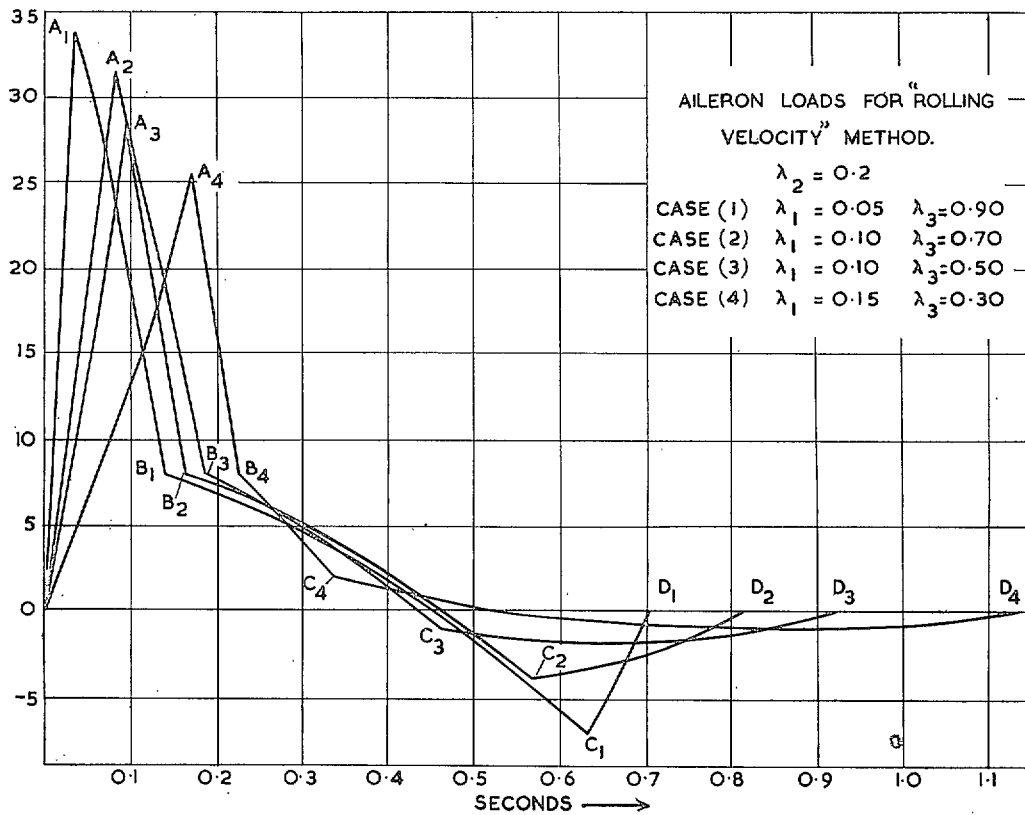


FIG. 10. Elevator co-ordination 'Good to Fair'.

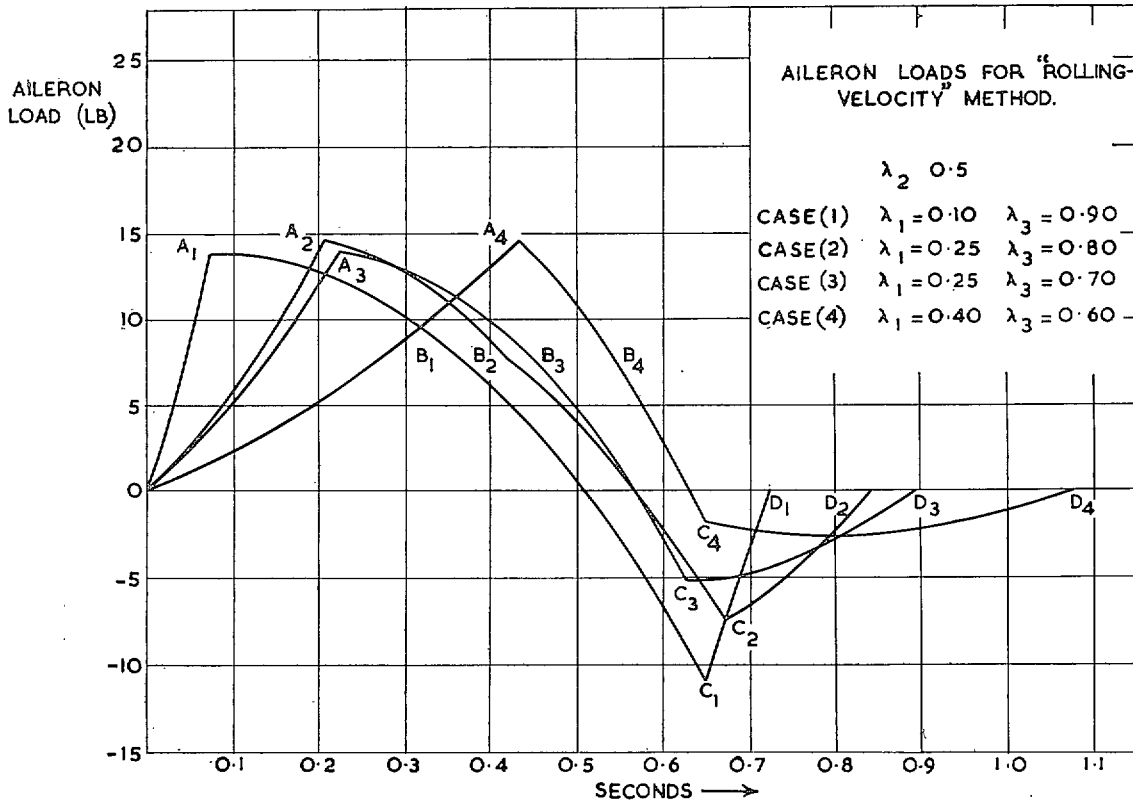


FIG. 11. Elevator co-ordination 'Fair to Poor'.

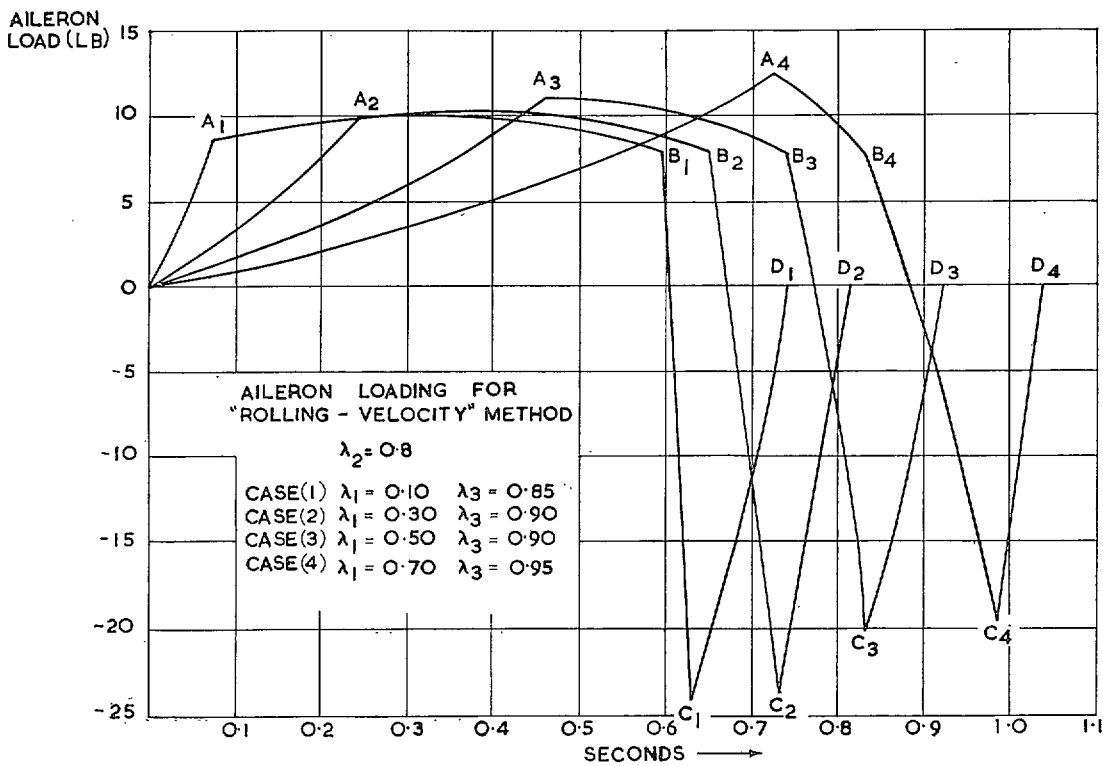


FIG. 12. Elevator co-ordination 'Very Bad'.

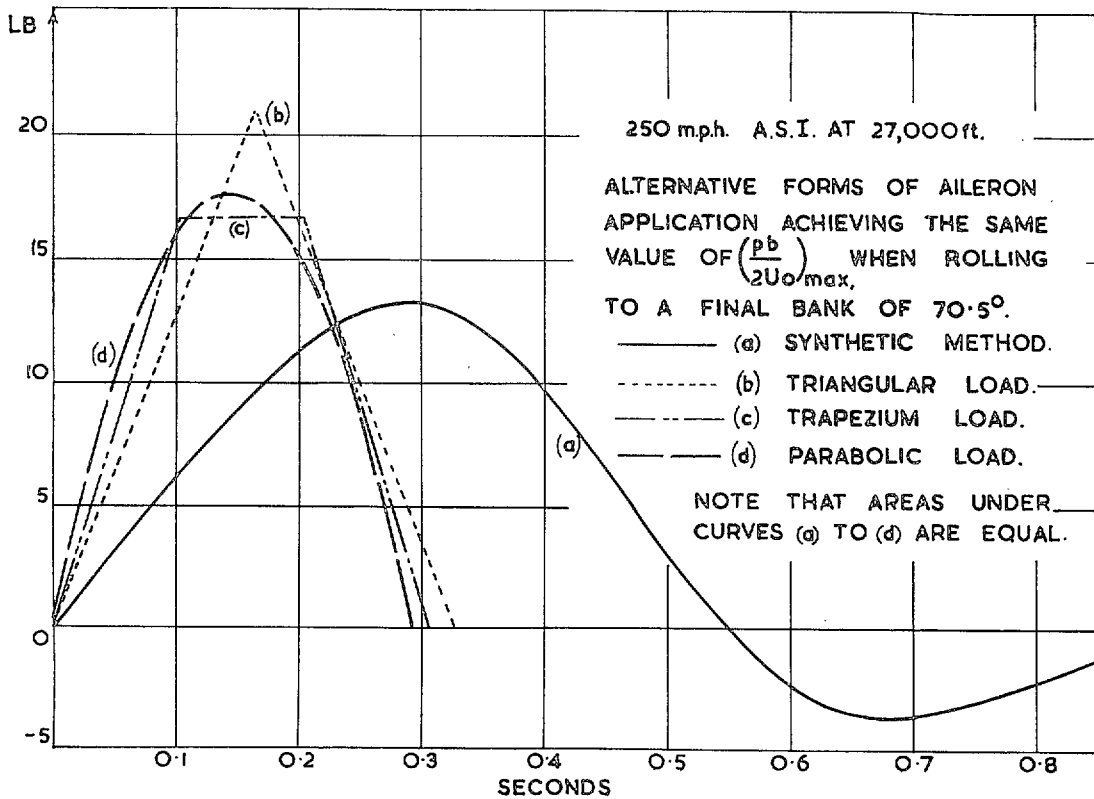


FIG. 13.

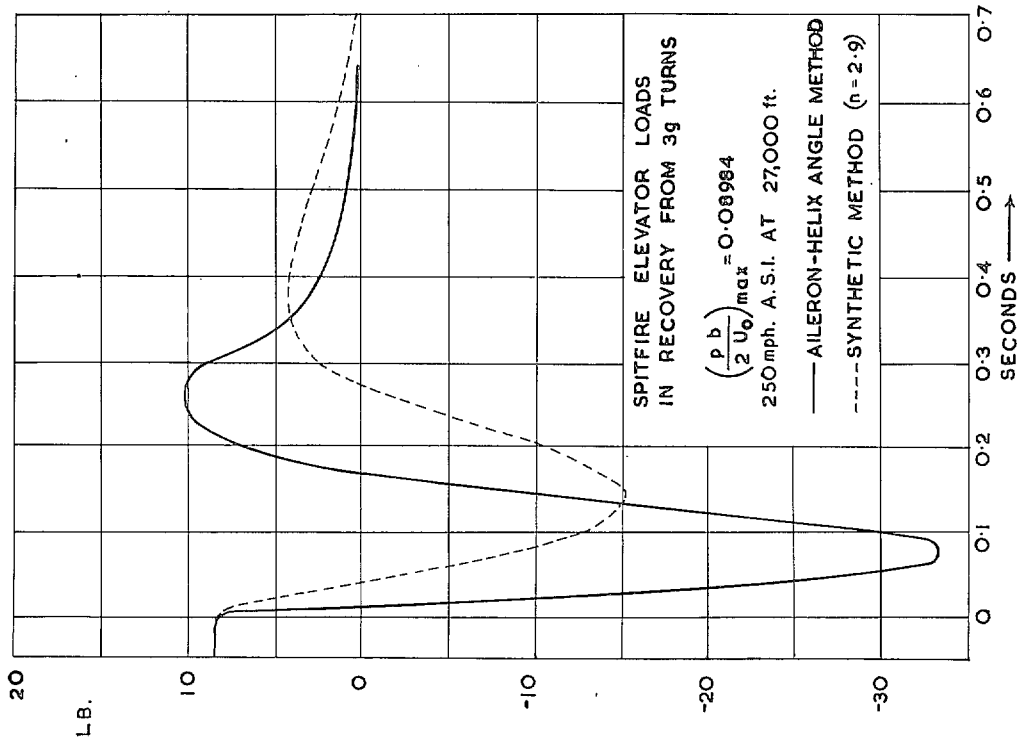


FIG. 14.

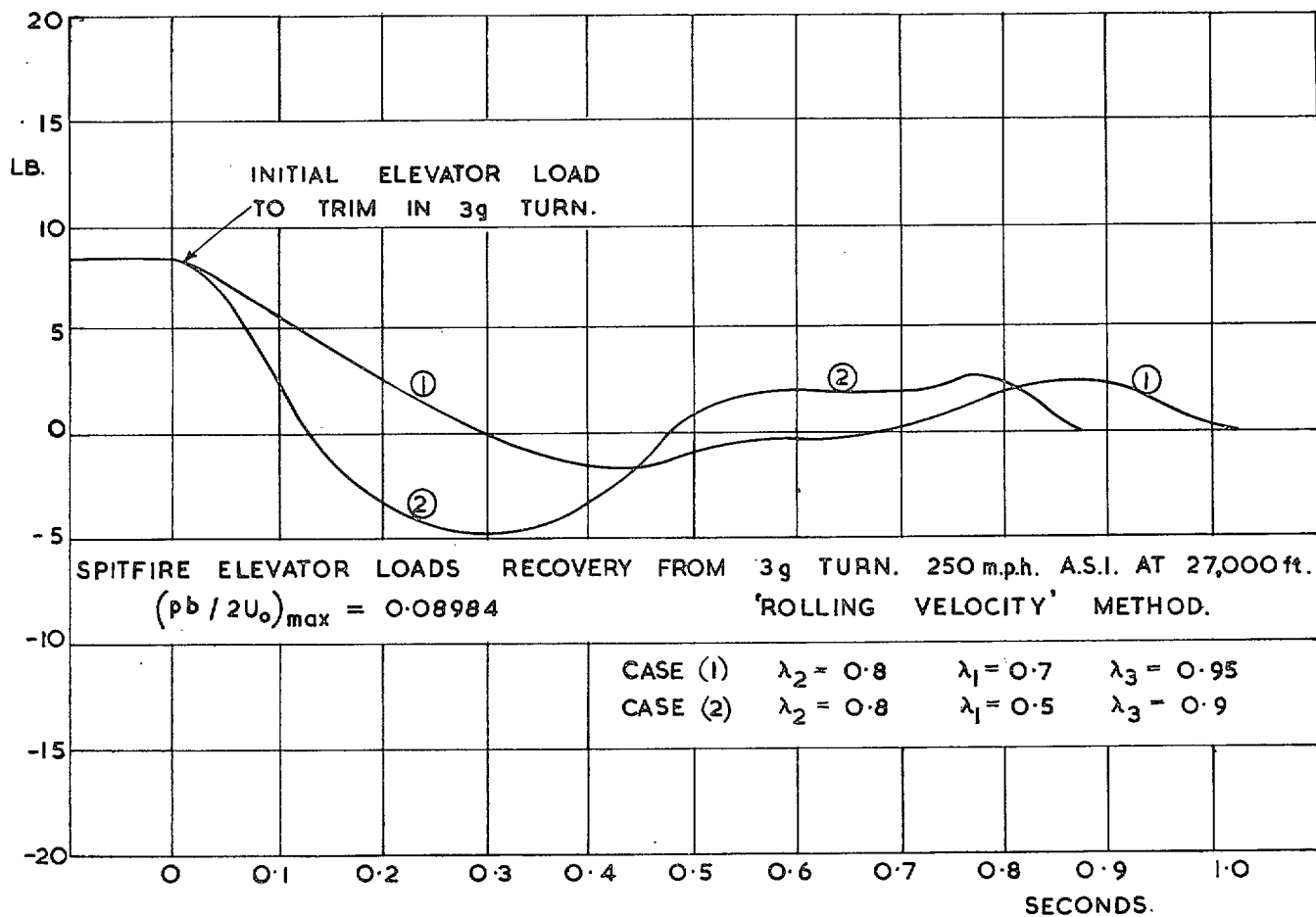


FIG. 15.

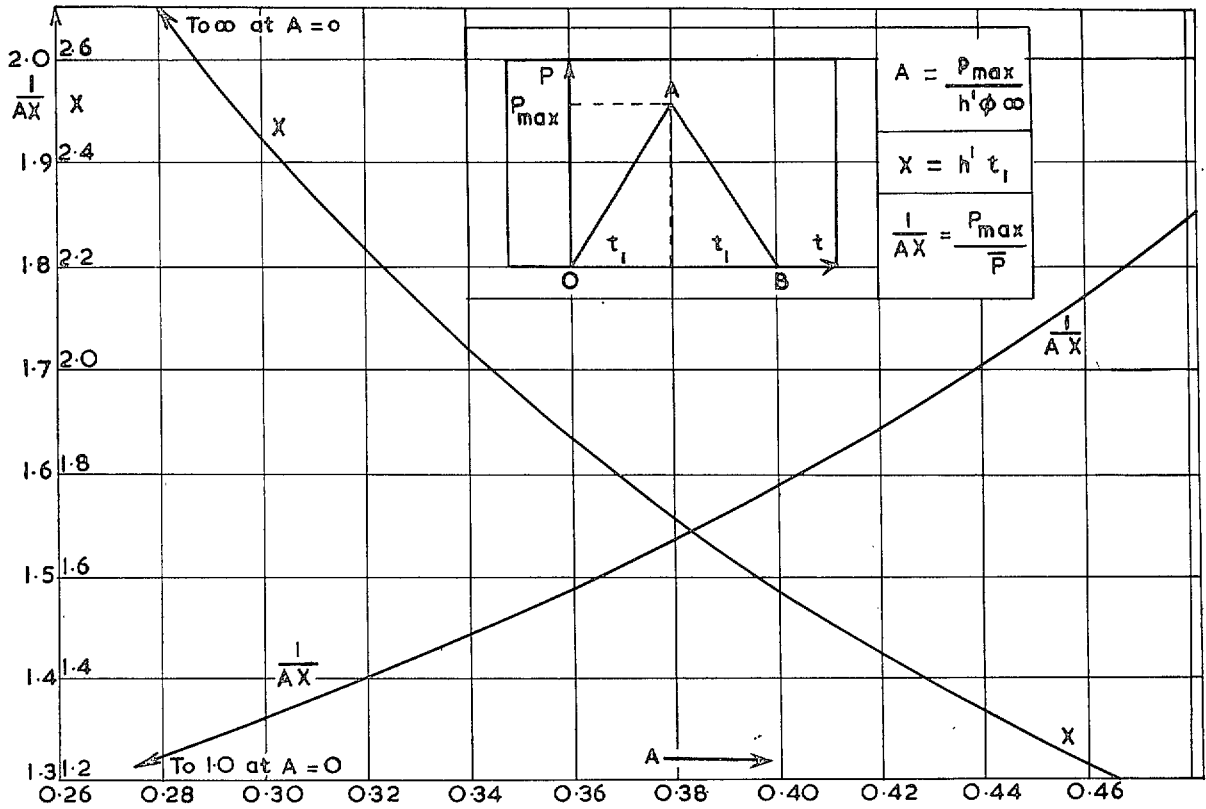


CHART I. Chart to determine aileron loads. Triangular loading.

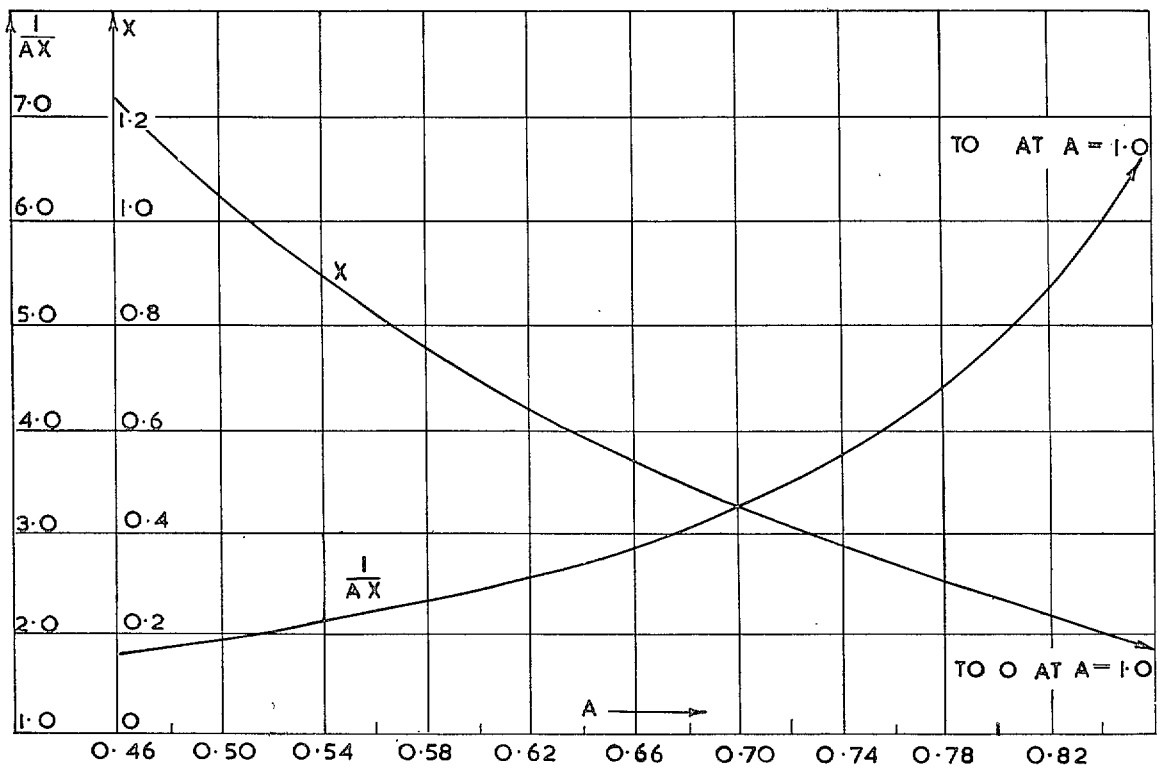


CHART I—continued.

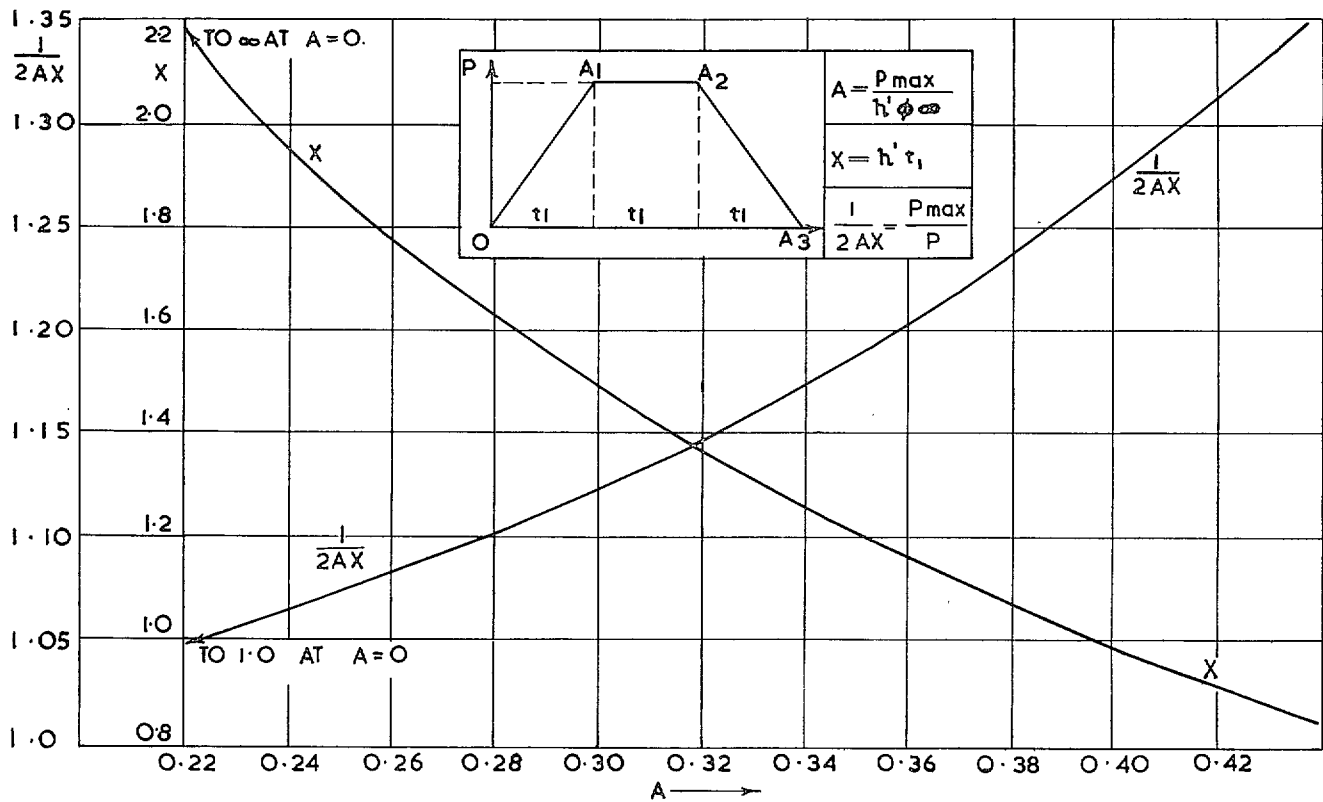


CHART II. Chart for determination of aileron loads. Trapezoidal loading.

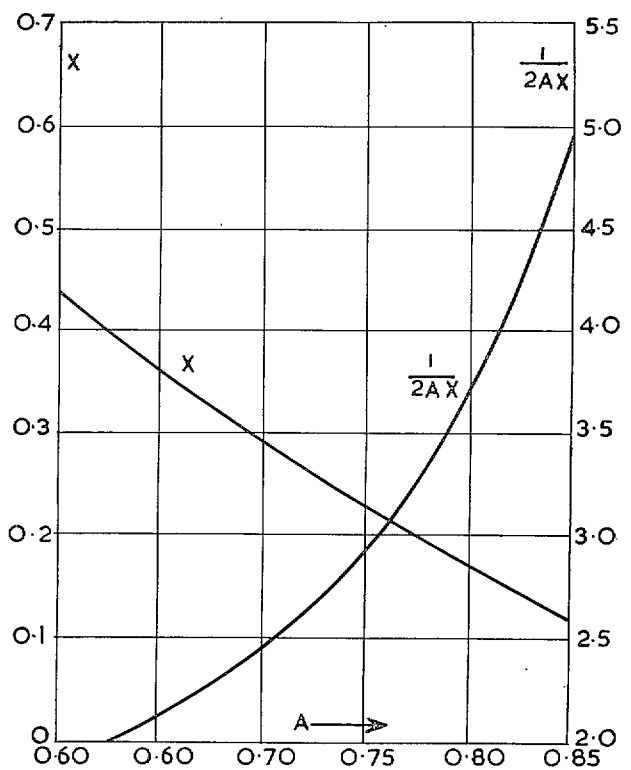
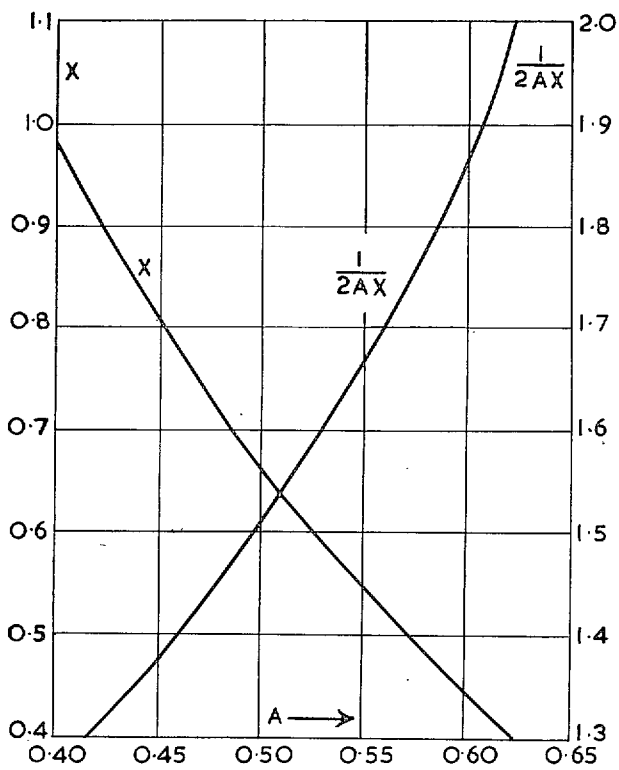


CHART II—continued.

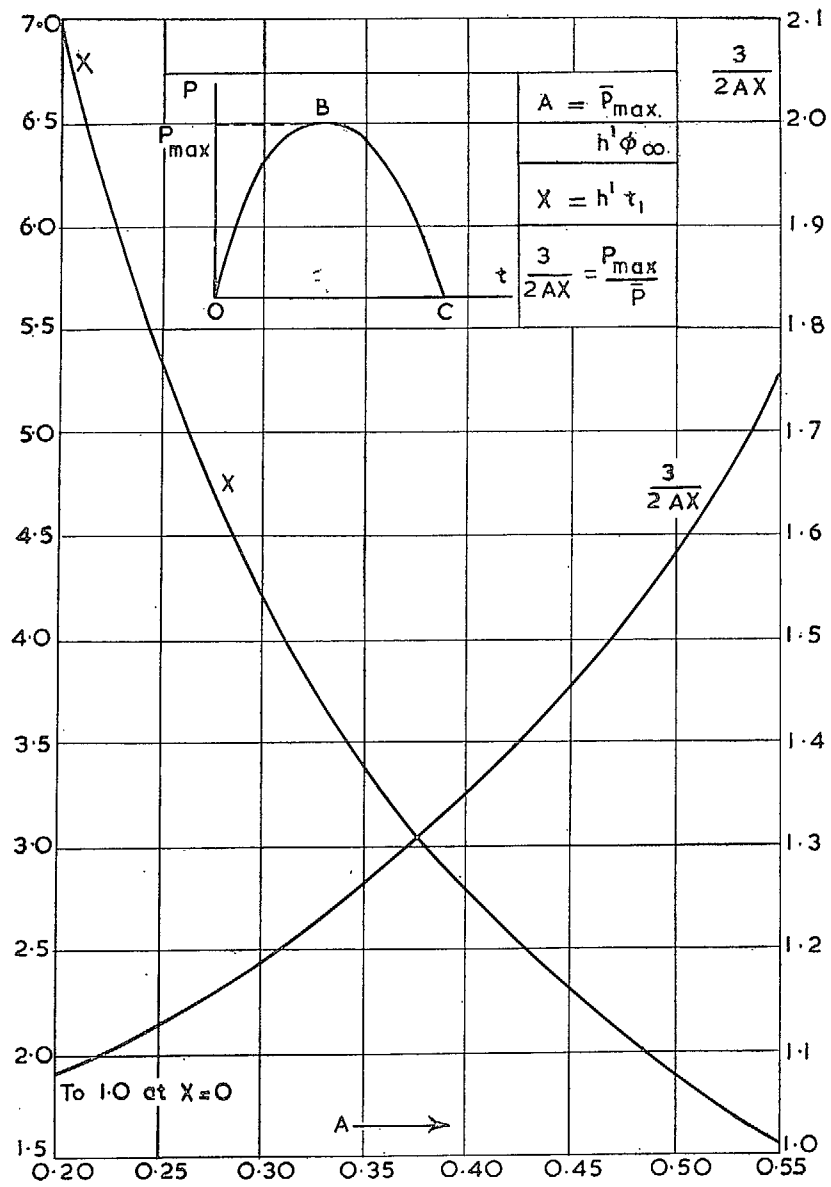


CHART III. Chart for determination of aileron loads. Parabolic loading.

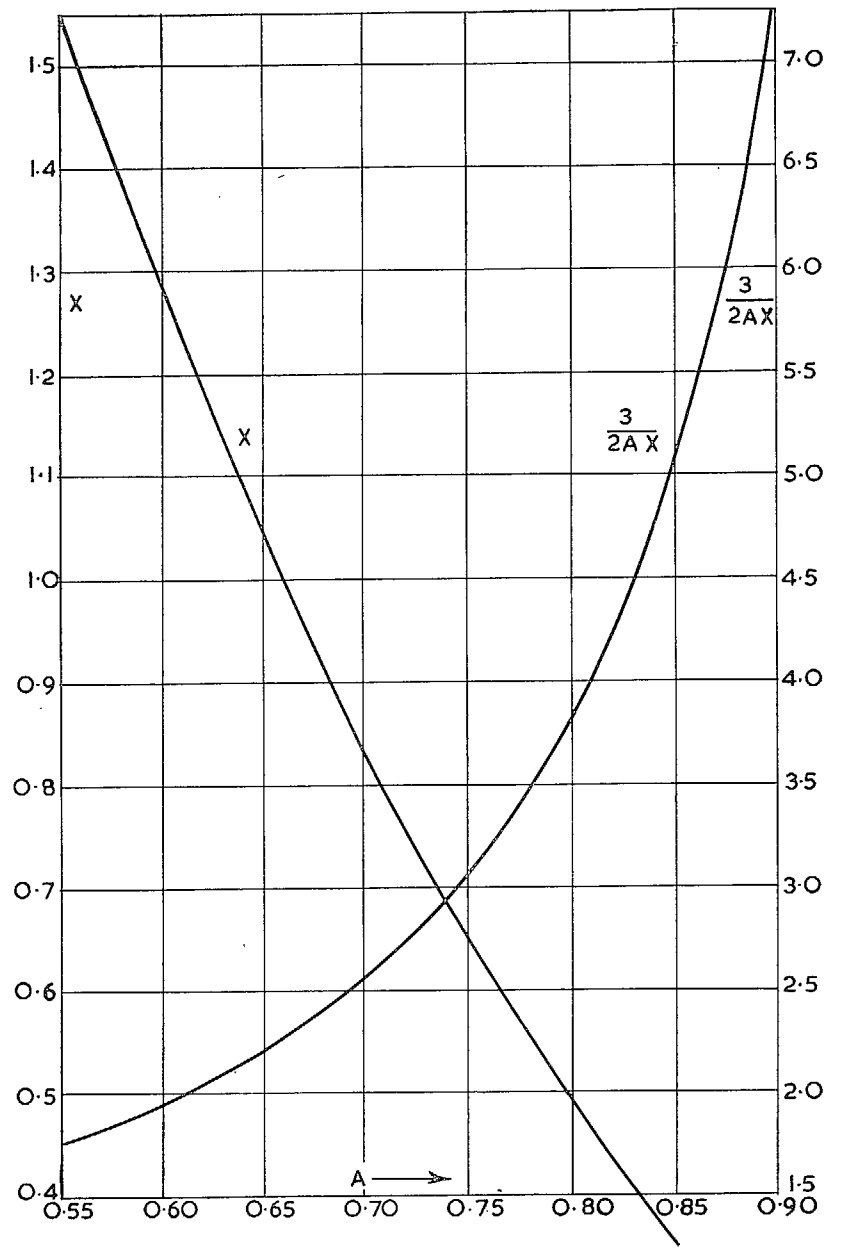


CHART III—continued

